

## Simulation of Vibrations in Electrical Machines for Hybrid-electric Vehicles

*Master's Thesis in the Automotive Engineering Master's Programme*

XIN GE

Department of Applied Mechanics  
Division of Dynamics  
CHALMERS UNIVERSITY OF TECHNOLOGY  
Göteborg, Sweden 2014  
Master's thesis 2014:12



MASTER'S THESIS IN AUTOMOTIVE ENGINEERING

Simulation of Vibrations in Electrical Machines  
for Hybrid-electric Vehicles

XIN GE

Department of Applied Mechanics  
*Division of Dynamics*  
CHALMERS UNIVERSITY OF TECHNOLOGY  
Göteborg, Sweden 2014

Simulation of Vibrations in Electrical Machines for Hybrid-electric Vehicles  
XIN GE

© XIN GE, 2014

Master's Thesis 2014:12  
ISSN 1652-8557  
Department of Applied Mechanics  
Division of Dynamics  
Chalmers University of Technology  
SE-412 96 Göteborg  
Sweden  
Telephone: + 46 (0)31-772 1000

Chalmers reproservice  
Göteborg, Sweden 2014

Simulation of vibrations in Electrical Machines for Hybrid-electric Vehicles  
Master's Thesis in the Automotive Engineering Master's Programme

XIN GE

Department of Applied Mechanics  
Division of Dynamics  
Chalmers University of Technology

ABSTRACT

Electric machines convert electrical energy into mechanical energy to provide the second source of power of a Hybrid Electric Vehicle. Electromagnetic forces are the most important source of vibration in Electric Machines. Therefore, the primary aim of the thesis is find out how to calculate this force excitation using the Finite Element method and estimate the vibration modes, resonance frequencies and sound pressure level by coupling it in ANSYS Workbench to understand how the electromagnetic force interaction with its mechanical structure. The secondary aim is to study the influence of the stator structure parameters and operating points using a sensitivity analysis. This report presents the simulation process and results of the vibration in this electric motor in ANSYS. The provided solution is being compared with the experimental data to estimate the accuracy of the simulation and the influenced factors are analyzed to optimize the structure to improve the vibration and acoustic performance of the electric machine.

Key words: ANSYS, Electromagnetic force, Vibration response, Resonance frequency, Acoustic performance, Electric machine



# Contents

ABSTRACT	I
CONTENTS	III
PREFACE	V
ACKNOWLEDGEMENT	V
NOTATIONS	VI
1 INTRODUCTION	1
1.1 Background	1
1.2 Objective	1
1.3 Literature Review	1
1.4 Simulation software: ANSYS	2
1.5 Research Process	4
2 ELECTROMAGNETIC FORCE CALCULATION	5
2.1 Maxwell Transient Solver	5
2.1.1 Maxwell equations	5
2.1.2 Solutions for Transient State Formulations	6
2.2 Electromagnetic analysis	7
2.3 Electromagnetic analysis	7
2.3.1 Electric machine 2D parameters	8
2.3.2 Boundary conditions and excitations	8
2.3.3 Mesh Operations	9
2.3.4 Simulation results	10
2.4 Parameters influence	12
2.4.1 Amplitude and phase angle	12
2.4.2 Air gap size	13
2.4.3 Eccentricity	14
2.4.4 Stator teeth thickness and tip width	15
3 ANSYS SIMULATION PROCEDURE	17
3.1 Vibration analysis settings	18
3.1.1 Material properties	18
3.1.2 Mesh generation	18
3.1.3 Load and boundary conditions	18
3.1.4 Contacts	19
3.2 Acoustic settings	20
4 VIBRATION AND ACOUSTIC PERFORMANCE	22
4.1 Stator vibration and noise	23
4.2 Influence of operating points	27

4.3	Structure influence	30
4.3.1	Cooling system shell	31
4.3.2	Windings	35
4.4	Rotor eccentricity	37
4.5	Experimental results	37
5	SENSITIVITY ANALYSIS	40
5.1	Local sensitivity analysis method	40
5.2	ANSYS Sensitivity analyse method	41
5.3	Local sensitivity analyse results	41
6	CONCLUSION	45
6.1	Discussion	45
6.2	Future scope	46
7	REFERENCE	47
8	APPENDIX 1	50
	APPENDIX 2	52
	APPENDIX 3	54
	APPENDIX 4	56

## Preface

This present thesis has been carried out at the Advanced Technology & Research within the Electromobility sub-systems group of Volvo Group Truck Technology in cooperation with Division of Dynamics in Department Applied Mechanics, at Chalmers University of Technology. The whole project has been carried out from January 2014 to June 2014. The supervisors of this master work are Pär Ingelström who at Volvo and Viktor Berbyuk and Håkan Johansson at Chalmers. The examiner of this project is Prof. Viktor Berbyuk.

## Acknowledgement

First of all, I would like to thank my supervisor Pär Ingelström who has always been there to help me with different problems. He gave me support on the simulation software ANSYS Maxwell and the operating principle of the electric machine used in this thesis work as well as practical issues.

I would also like to give thanks to Dan Hagstedt and Mats Strådalén for providing me a CAD model of the machine and the structure parameters. Besides, this thank is given to Zhe Huang who always discussed with me with several questions and ‘saved the world’ every time.

Furthermore person I would like to thank is all the staff doing the experiment to test the vibration and acoustic response of the machine and giving comments on the part which should be paid most attention to, though I do not know the name of all the people accomplished this test.

These thanks must give to my examiner Viktor Berbyuk and my supervisor Håkan Johansson who arranged the meeting every time and came to the company to help me with the problems I had during the simulating time, as well as giving opinions and reading my paper. And also my thanks will give my opponent in the final presentation Squires Joshua.

Last but not least, I would like to thank everyone who helped me in this short time thesis work in my one year study in Chalmers University. They are Lennart Josefson, Martin West and Anders Fredén.

Göteborg May 2014

Xin GE



# Notations

The following list is all the variables and abbreviations in this paper which is provided for a better reading of the whole passage.

## Symbols

$\nabla$	Gradient operator
$\nabla \cdot$	Divergence operator
$\nabla \times$	Curl operator
$\nabla^2$	Laplace operator

## Roman upper case letters

$A$	Magnetic vector potential	$V \cdot s/m$
$B$	Magnetic flux density	T
$B_n$	Normal component of flux density	T
$B_t$	Tangential component of flux density	T
$c$	Damping coefficient	Ns/m
$D$	Electric flux density	$C/m^2$
$E$	Electric field intensity	V/m or N/C
$E(material)$	Young's Module	Pa
$F_{rad}$	Radial electromagnetic force	N
$F_{tan}$	Tangential electromagnetic force	N
$G$	Shear modulus	
$H$	Magnetic field intensity	A/m or T
$H_c$	Coercive magnetic field intensity	A/m or T
$L_{stk}$	Stack length of the motor	m
$J$	Current density	$A/m^2$
$k$	Spring coefficient	N/m
$V$	Electrical scalar potential	V
$SPL$	Sound pressure level	dB
$X_0$	Maximum static displacement	m

## Greek lower case letters

$\sigma$	Electric conductivity	S/m
$\sigma(material)$	Normal stress	Pa
$\varepsilon$	Electric permittivity	F/m
$\varepsilon(material)$	Forward strain	
$\varepsilon_0$	Electric permittivity in free space	
$\varepsilon_r$	Relative permittivity	
$\mu$	Magnetic permeability	$W_b/A \cdot m$
$\mu_0$	Magnetic permeability in free space	
$\mu_r$	Relative permeability	
$\rho$	Electric charge density	$C/m^3$
$\zeta$	Damping ratio	



# 1 Introduction

This chapter gives an introduction of the thesis background as well as a literature review of the recent research in vibration and noise of electric machines. A brief introduction of the simulation software used in this thesis work and the main objectives will sum up this chapter.

## 1.1 Background

Fuel prices in the world nowadays are about 4 times of that in 2000. For example, the cost of gasoline in Sweden has risen by about 2 times in the past 20 years. At the same time, gasoline is a non-renewable resource, whose reserves are getting reduced day by day. Due to these problems, a hybrid vehicle that consists of two different sources of power which are internal combustion engine and electric motor makes more economical and environmental sustainable sense, because it offers great energy efficiency, energy recovery, less dependence on conventional fuels and lower exhausted emissions. Hybrid electric vehicles are developed rapidly in recent years. The demands on electrical motors for HEVs differ greatly from those on traditional industrial electrical motors, especially when it comes to power density. However, pushing torque and speed towards the limit also means that noise and vibrations will increase. Simultaneously, the machine should be ideally noiseless, lighter, and more user-friendly.

An electrical machine in a HEV converts electrical energy into mechanical energy and vice versa. The magnetic field in the air gap between the stator and rotor in the electric motor generates tangential forces required for producing the rotating torque. In addition, this magnetic field also produces radial forces that interact with the machine structure and create the vibration and noise. Research and simulations of vibrations of large electric machines have been done for several years.

## 1.2 Objective

This thesis focuses on the vibration of an electric machine prototype developed at Volvo for hybrid vehicle applications, which will be divided into two parts. One part is the vibration mode and resonance frequency of the stator and rotor. Based on the calculation of electromagnetic forces by ANSYS Maxwell, the force excitation will be used as the applied force in ANSYS Mechanical to simulate the vibration modes as well as sound level pressure for different models of the electric machine, such as the stator vibration model under different operating torque. Then compare the simulated results with the experiment data to get the main concerned frequency range of the vibrations. The second part is the sensitivity analyzes of the structure parameters of the machine. This includes the outer diameter of the stator, thickness of shell, thickness of yoke and air gap. Based on the analyze results, the electric machine structure can be optimized to achieve less vibration and higher resonance frequencies.

## 1.3 Literature Review

Electromagnetic force is the most important vibration source for stator in an Electrical Machine. A combination with experiment and simulation method is used to estimate the vibration response and find existed problems of the remaining design. Researches have been done on the force excitation as well as vibration mode analysis of inducted motors and ultrasonic motors. The magnetic field distribution and transient characteristics of a surface permanent magnet brushless DC motor has been calculated

and is used to accurately estimate the features and noises of a PMSM. In addition, an optimal design method of minimizing the vibration and sound power level is proposed. Here, the electromagnetic force, mechanical vibration and noise emission is calculated from a linear analytical model. Furthermore, the influence of connection way between slots and groove as well as carrier frequency to acoustic performance has been researched by an experiment. It shows that fractional windings may cause the increasing of the vibration and noise of the PMSM, but changing the carrier frequency can effectively inhibit the noise and vibration level.

Besides, tests focused on how the end of slots, rotor structure and operating conditions affect the natural frequency of EM system have been carried out in 1989. William Cai and P Pillay (2001, 2002) studied the influences of chassis, heat sink and outlet box on the intrinsic mode of the stator for a switched reluctance motor. It pointed out that the length of stator core as well as chassis has small effects on the stator plane modes, whereas the thickness of stator core and cabinet has great impacts on the natural frequency of the system. Among them, heat sink and outlet box downsize the low natural frequency and upsurge the high resonance frequency. Also, the three vibration types are pointed out which are radial, axial and torsional vibration. Among them, axial vibration is rare, except for a large electrical machine. Torsional one may occur in the motor with salient poles or skewed slots.

However, most of these researches and experiments were done for traditional motors with large size and low power which has different structure with the EM on a Hybrid vehicle. Therefore, in this thesis project, an electrical machine prototype of a HEV is simulated.

## **1.4 Simulation software: ANSYS**

The Finite Element Method is a numerical tool for analyzing structures and continua as well as solving problems of engineering and mathematical physics. These problems often concern stress analysis, heat transfer, fluid flow, vibrations, electric and magnetic fields and several other areas which are used in the design of buildings, engines, electric motors, cars, etc. FEM is a method for converting a partial differential equation into systems of algebraic equations, which are well suited for being solved with computers.

Finite element analysis using commercial software such as ANSYS involves several steps.

First, build or import the geometry of the model which will be simulated and divide this structure into finite elements. What is more, set the properties of those elements to obtain a suitably fine mesh for the simulation. Then apply the load like forces, torque, velocity on the exact point. Also the support method needs to be specified such as cylinder support, fixed support. Finally, solve the model under different settings and achieve the results.

Compared with analytical method, numerical method like FEM achieves the exact data, arbitrary shape, loads which makes the result more specified and visualized. Also the model is not simply an abstraction. It seems almost true in structural mechanics. Besides, user can define many boundary conditions who make the model similar to the real operating environment.

However this method also has disadvantages. One specific numerical analysis provides no-closed-form solution that permits simulation under changing various

parameters. The storage and CPU also has to be strong enough to this calculation. And those models are always simplified in order to shorten the simulation time which will lead the inaccuracy of the results.

ANSYS is a software using FEM to solve differential equations. The main simulation technology includes Structural Mechanics, Systems and Multiphysics, Electromagnetics, Fluid Dynamics, Explicit Dynamics and Hydrodynamics. The workflow technology involves ANSYS Workbench Platform, High-Performance Computing, Geometry Interfaces and Simulation Process and Data Management.

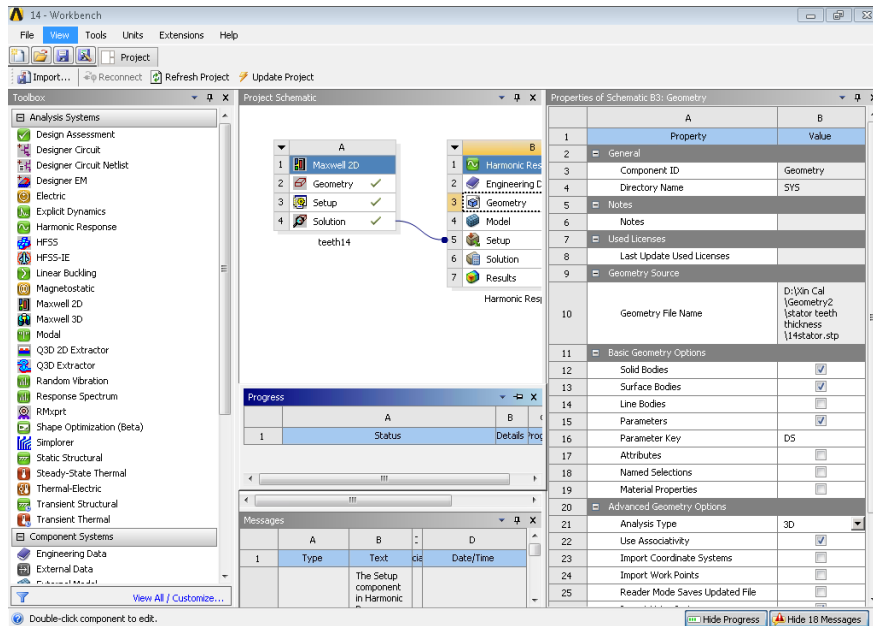


Figure 1.1 ANSYS Workbench interface

ANSYS analysis system consists of modal analysis, harmonic-response analysis, response-spectrum analysis, random-vibration analysis and transient analysis shown in Figure 1.1. Modal analysis can be used to determine a structure's vibration characteristics, i.e., mode shapes and natural frequencies. Harmonic-response analysis can be used to determine a structure's response to sinusoidally varying, steady loads like rotating machines which exert steady, alternating forces on bearings and support structures. A response-spectrum analysis is used to determine how one component responds to earthquakes. For example, skyscrapers, cooling towers of power-plant and other structures must withstand multiple short-duration transient impact loadings which is common in seismic events. A random-vibration analysis is used to determine how one component responds to random vibrations. For instance, aircraft and spacecraft components must withstand random loadings of varying frequencies in a sustained time period. Transient analysis can be used to simulate a structure's response to time varying loads.

In this thesis work, the electromagnetic force is the excitation load which is a sinusoidally-varying excitation across a range of frequencies and the out parameter is the deflection of the structure that is a sinusoidally-varying response at each corresponding natural frequency. Therefore, harmonic response analysis is used to simulate the vibration response of the electric machine.

ACT\_Acoustics, an extensional analyzing model for exposing 3D acoustic features in ANSYS Mechanical without the need for APDL. It is a customization made model with ACT to integrate ANSYS acoustics capability in Mechanical. The extension

consists of one XML file that configures the UI content and one python script which implements the extension functionality. It is a study of the generation, propagation, absorption and reflection of sound pressure waves in a fluid medium. This can be applied to sonar - the acoustic counterpart of radar, noise minimization in automobiles, underwater acoustics and design of concert halls, where an even distribution of sound pressure is desired, geophysical exploration and so on. This will be used in calculating the SPL of the electric machine.

## **1.5 Research Process**

This thesis work is divided into 4 major parts: establishing the project, building the model and evaluation, experiment validating and concluding with paper writing.

The first phase consists of literature review of the recent thesis paper and tutorial studying of ANSYS. The basic working principle of the electric machine, the flowchart of simulation process, the operation of ANSYS Maxwell as well as Mechanical will be done within this period. Then build the 3D model of the motor and simulate the vibration and acoustic response using Harmonic Response analysis, as well as analyze the simulating results in the second phase which concerns the major part of the project. After finishing these works, compare the calculation data with the experimental result. The main conclusion is not the optimization of the design of the electric machine, but the influence of the parameters (sensitivity analyze) which can be further calculate in the future work.

## 2 Electromagnetic force calculation

The amplitude of the vibrations and the SPL (Sound Pressure Level) at any position is mainly depend on the varying forces acted on the structure, but also on the mechanical response, the characteristics and the assembly of the machine. Those forces cause vibrations in the structure of the electric motor. What is more, the vibrations will be transmitted in the surrounding media. The vibration forces can be divided into three groups which are electromagnetic force, mechanical force and air friction force. The electromagnetic force and rotating torque which will provide the power to drive the electric machine is produced in the magnetic field in the air gap. And the most important magnetic force producing vibrations of the motor is due to the flux in the air gap. Magnetic flux can cross the interface between an infinitely permeable and a vacuum medium and only in a vertical direction to the surface. Finite Element Method is used to calculate the magnetic flux scattering of the Electric Machine, then the harmonic electromagnetic forces will be calculated by ANSYS Maxwell Stress Method and Fourier Analysis. These forces are subsequently used as the applied force in the simulated stator model to study the vibrations of different models.

### 2.1 Maxwell Transient Solver

ANSYS Maxwell is a commercial interactive software using the Finite element methods to solve electric and magnetic problems. It determines the electromagnetic field by solving Maxwell's equations within a finite region of space with user-defined initial conditions and appropriate boundary conditions.

#### 2.1.1 Maxwell equations

The complete set of equations is shown as below:

$$\nabla \times E = -\frac{\partial B}{\partial t} \quad (2.1)$$

$$\nabla \cdot B = 0 \quad (2.2)$$

$$\nabla \times H = J + \frac{\partial D}{\partial t} \quad (2.3)$$

$$\nabla \cdot D = \rho \quad (2.4)$$

where  $E$  is the electric field intensity,  $B$  is the magnetic flux density,  $H$  is the magnetic field intensity,  $J$  is the surface current density,  $D$  is the electric flux density and  $\rho$  is the volume charge density. For stationary and quasi-stationary electromagnetic field distribution situations, the displacement current density  $\frac{\partial D}{\partial t}$  is neglected, which gives the equation:

$$\nabla \times H = J \quad (2.5)$$

In three dimensions, when the divergence of the curl of any vector field is equal to zero, the following equation can be obtained:

$$\nabla \cdot J = \nabla \cdot (\nabla \times H) = 0 \quad (2.6)$$

The properties of macroscopic material are defined by the constitutive relations who are shown as below:

$$J = \sigma E \quad (2.7)$$

$$D = \varepsilon E = \varepsilon_0 \varepsilon_r E \quad (2.8)$$

$$B = \mu H = \mu_0 \mu_r H \quad (2.9)$$

Here,  $\sigma$  is the electric conductivity,  $\epsilon$  is the electric permittivity which is given as  $\epsilon_0 * \epsilon_r$ , where  $\epsilon_0$  is the permittivity in free space and  $\epsilon_r$  is the relative permittivity that determines the electric field solution in the insulators. It can be simple or anisotropic.  $\mu$  is the magnetic permeability,  $\mu_0$  is the permeability in free space and  $\mu_r$  is the relative permeability along with the magnetic coercivity determine the magnetic properties of the material. It can be simple (linear) or nonlinear (BH Curve) or anisotropic.

### 2.1.2 Solutions for Transient State Formulations

Appropriate set of equations and their terms are used based on the selecting solvers, such as Maxwell static solver, eddy current and transient solver. Electric and magnetic transient solver solves different transient fields.

Magnetic transient solver computes time varying magnetic fields. It is a time domain solver which solves for instantaneous magnetic fields at each time step. The sources of time varying magnetic field can be moving sources, moving permanent magnets and time-varying voltages or current sources in linear or nonlinear materials. Furthermore, the induced fields such as proximity and skin effects are considered. Electric transient solver computes time varying electric fields caused by time-varying voltages, charge distributions or applied current excitations in inhomogeneous materials. Electrical potential is the solution quantity. But this solver is only available in 3D Maxwell simulation.

To simulate the process of converting electric energy into mechanical energy in 2D Maxwell, magnet transient solver is used in this electric machine simulation.

$A$  is the magnetic vector potential that is defined as:

$$\nabla \times A = B \quad (2.10)$$

It is defined in the whole problem region and can be coupled with the electric scalar potential  $V$  which is defined by:

$$E = -\frac{\partial A}{\partial t} - \nabla V \quad (2.11)$$

For the electric scalar potential, one high value and low value of  $V$  are defined separately at the two ends of the conducting region. But  $V$  equals to zero at the non-conducting region. Therefore, combining equations (2.5), (2.7), (2.9), (2.10) and (2.11), the magnetic flux density  $B$  and current density  $J$  can be calculated.

$$J = \sigma E = -\sigma \left( \frac{\partial A}{\partial t} + \nabla V \right) = \nabla \times H = \nabla \times \frac{B}{\mu} = \frac{1}{\mu} \nabla (\nabla \times A) \quad (2.12)$$

By using Coulomb Gauge,

$$\nabla \cdot A = 0 \quad (2.13)$$

The transient state formulations for electromagnetic field will get the solution as shown in equation (2.14).

$$\nabla \times \left( \frac{1}{\mu} \nabla \times A \right) = \nabla \times H_c - \sigma \left( \frac{\partial A}{\partial t} + \nabla V \right) + \frac{1}{\mu} \nabla (\nabla \cdot A) \quad (2.14)$$

Here,  $H_c$  is the coercive magnetic field intensity.

## 2.2 Electromagnetic analysis

There are three types of magnetic force existed in an electrical machine. They are reluctance force that acts on the material boundaries with different magnetic properties, Lorentz force which acts on windings in the magnetic field and magnetostrictive force acting inside the iron core. The most important vibration excitation is the reluctance force produced in the air gap between the stator and rotor because of the larger magnitude and the less complexity compared with the other forces.

The reluctance force of electric motor is electromagnetic force which has two components, radial and tangential components. In a two dimensional FEA calculation, the material boundaries are chosen as the edge of stator tip. The two components of electromagnetic force can be calculated according to equation (2.15) and (2.16):

$$F_{rad} = \frac{L_{stk}}{2\mu_0} \oint_l (B_n^2 - B_t^2) dl \quad (2.15)$$

$$F_{tan} = \frac{L_{stk}}{\mu_0} \oint_l B_n \cdot B_t dl \quad (2.16)$$

where  $B_n$  and  $B_t$  is the normal and tangential component of flux density respectively,  $l$  is the length of the stator tip edge and  $L_{stk}$  is stack length of the machine.

Machines having diametrically asymmetric disposition of air gap is called eccentricity when the center of rotor and stator is not coincident. This often causes the undesired force waves and the electromagnetic force excitation will be unpredictable.

## 2.3 Electromagnetic analysis

The Maxwell 2D electrical machine consists of two main parts which are stator part contacted with windings as well as rotor part included magnets and rotor shaft as is shown in Figure 2.1.

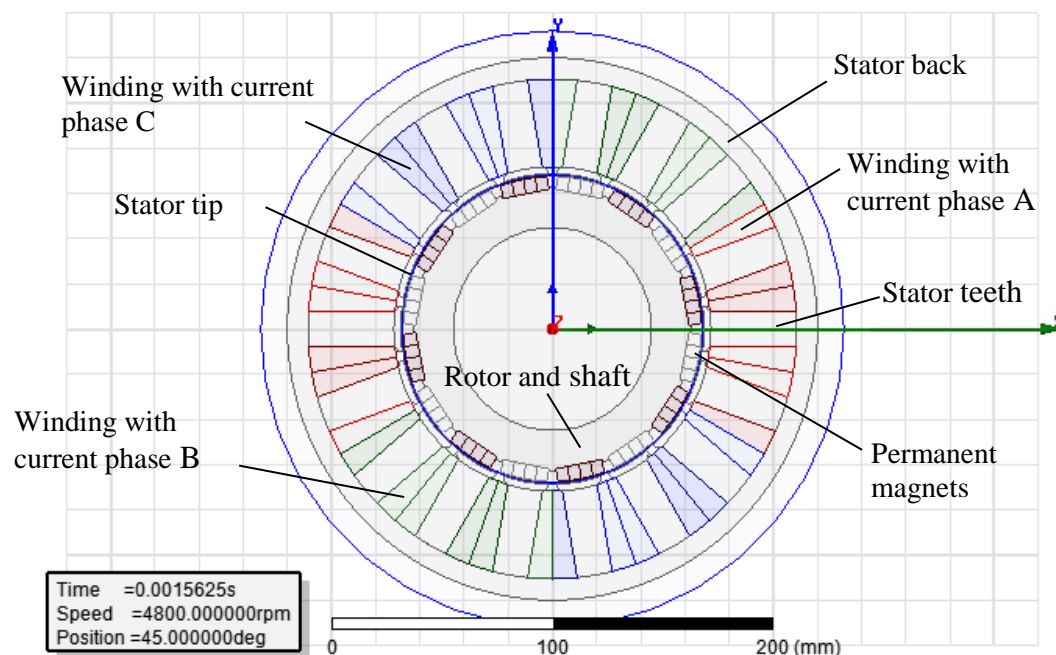


Figure 2.1 Maxwell 2D model of Electrical machine

### 2.3.1 Electric machine 2D parameters

The specific structure parameters of the 2D electrical machine and the operating points for this model are shown in Table 2.1.

Table 2.1 Geometry parameters and operating points of the simulated machine

Parameters	Value	Unit
Stator inner radius		mm
Stator outer radius		mm
Rotor radius		mm
Thickness of one stator teeth		mm
Total number of teeth		
Yoke thickness	1,5	mm
Air gap	1,2	
Electric frequency (efreq)	640	Hz
Rotating speed	4800	rpm
Amplitude of current $I_s$	92,2	A
Phase angle $\theta_A$	141,4	deg
Current A	$I_s \cdot \sqrt{2} \cdot \sin(2\pi \cdot \text{efreq} \cdot t + \theta_A)$	
Current B	$I_s \cdot \sqrt{2} \cdot \sin(2\pi \cdot \text{efreq} \cdot t + \theta_A - 120)$	
Current C	$I_s \cdot \sqrt{2} \cdot \sin(2\pi \cdot \text{efreq} \cdot t + \theta_A - 240)$	

### 2.3.2 Boundary conditions and excitations

This is a Permanent Magnet Synchronous Motor (PMSM). A constant magnetic field created by the permanent magnets interacts with the rotating magnet field generated by the three-phase alternating current and thus rotating torque is produced on the rotor. Rotor rotates at the synchronous frequency corresponding to the electric frequency of the input current as shown in equation 2.17. The 3-phase AC current are sinusoidal waves and always sum up to be zero at any time. The input current excitations and induced voltage are shown in Figure 2.2.

$$f_{electric} = \frac{P}{2} \cdot f_{mechanical} \quad (2.17)$$

From the Fast Fourier Transform results, the electrical current frequency happens at 640Hz as the input value, but the induced voltage has other harmonics except for the sinusoidal wave and the frequency happens at 1920Hz and 3200Hz which is 3 times and 5 times of the electric frequency.

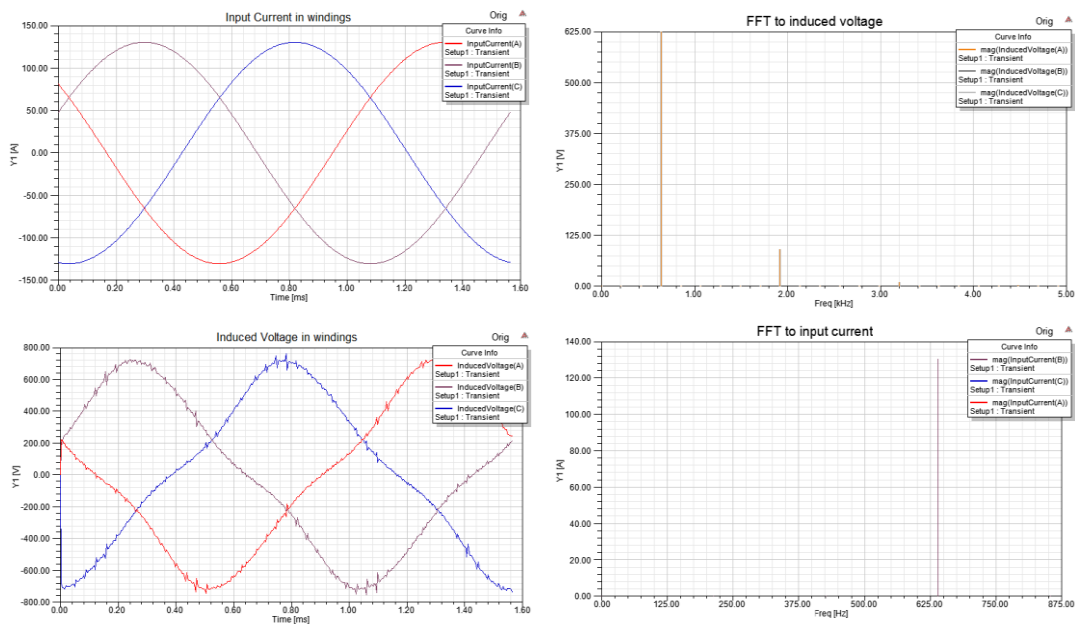


Figure 2.2 Input current, Induced voltage and FFT results

The zero vector potential boundary condition is applied to the boundary lines of the whole stator part. And rotor part is defined as a rotating structure. It determines that all magnetic flux lines are tangential to this solution region boundary. These lines reflect lamination-surrounding air interface which represents very significant step change of material parameters. Therefore, the magnetic force lines cross this boundary to a very limited extent which means a magnetically isolated structure.

### 2.3.3 Mesh Operations

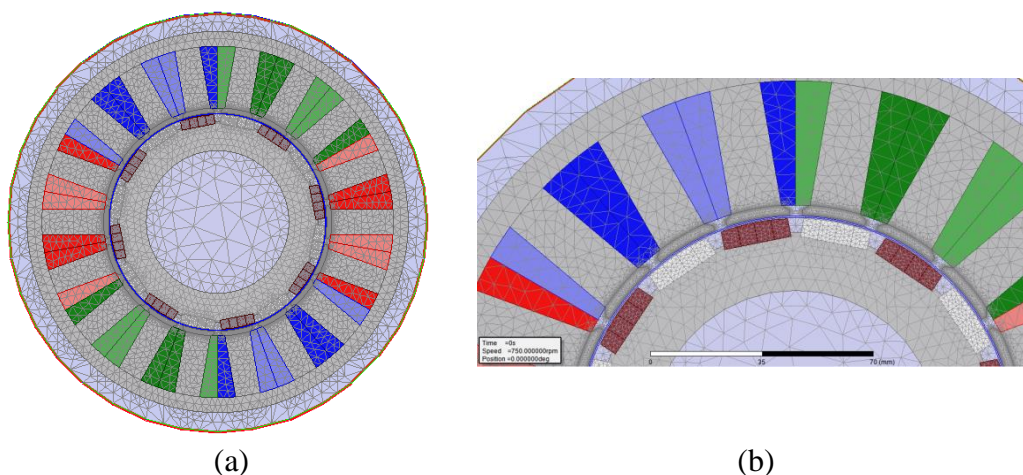


Figure 2.3 Mesh generation of 2D model

Mesh plays an important role in the accuracy of calculating results and thus requires meshes with higher resolution in regions where these fields are varying rapidly. ANSYS Maxwell provides six mesh operation specifications. In this project, On selection length based mesh operation as well as surface approximation mesh

operation is used to specify the edges of windings, magnets, stator tips while the default triangles mesh is defined in the boundary region.

Length based on-selection refinement limits the edge length of all triangle meshes formed on the surface by controlling the maximum size and maximum count of the elements on the boundary. As shown in Figure 2.3(a), the maximum size of the triangle elements edge for windings, all steel parts, magnets and stator tips is defined as 8mm, 6mm, 2mm and 0.25mm respectively.

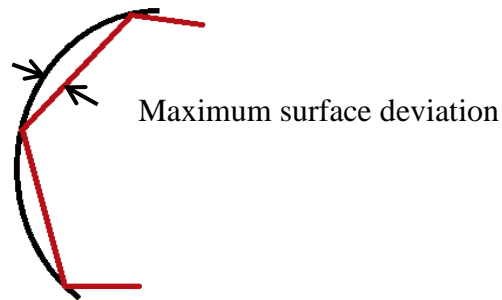


Figure 2.4 Maximum surface deviation definition

Here the surface approximation mesh operation is used to refine stator tip curve with a good quality mesh by increasing the mesh density since the radial electromagnetic forces are directly acted on the stator tips which cause the vibration of stator. The maximum surface deviation shown in Figure 2.4 is set as 0.005mm and the meshes are displayed as Figure 2.3(b).

### 2.3.4 Simulation results

Based on the basic definition of the parameters, meshes and boundaries, electromagnetic response for one cycle of rotor rotation is simulated in 3200 steps. The total simulation time is 12.5ms. Magnetic field generated by the alternating current interacts with the constant magnetic field created by permanent magnets and the flux lines of 45 deg rotor position are shown in Figure 2.5. These lines keep constant in this surface.

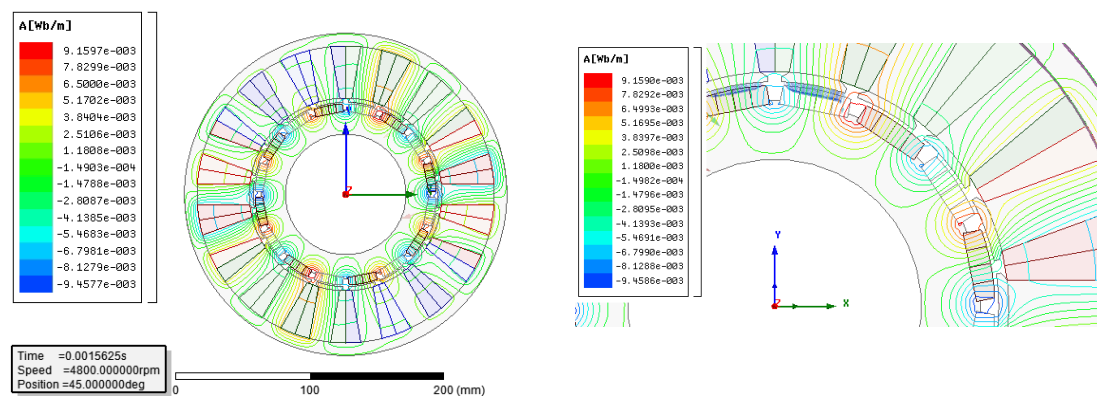


Figure 2.5 Magnetic flux lines for 45 deg rotor position

The magnetic flux density inside the unsaturated ferromagnetic material is very small compared to the flux distribution within air gap, hence, the electromagnetic force contributed on these parts is small. Because of the length-based meshing method, the edge force is calculated on the nodes of every edge elements, thus the electromagnetic force is defined as the integration of the edge force density for stator tips. Every edge force consists radial and tangential component which is calculated from the following

equations (2.18) and (2.19). What is more, the radial and tangential force curve for one time cycle of the current for the first six tips is shown in Figure 2.6.

$$F_r = F_x \cos \theta_{tip} + F_y \sin \theta_{tip} \quad (2.18)$$

$$F_t = -F_x \sin \theta_{tip} + F_y \cos \theta_{tip} \quad (2.19)$$

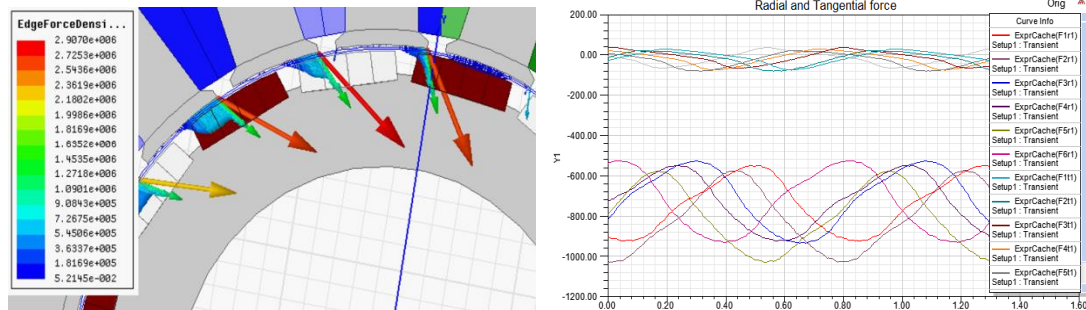


Figure 2.6 Radial and tangential forces for stator tip edges

Radial components of the forces perpendicular to every teeth tip cause the radial deformation and vibration. Meanwhile tangential parts acted on the rotor produce a rotating torque, nevertheless, tangential forces acted on stator cause unavoidable torsional deformation. From Figure 2.6, the magnitude of tangential force almost equals to zero, but amplitude of radial force is much greater than tangential part which means the unwanted vibration excitation is serious. Force wave acts on the first and fourth, second and fifth, third and sixth shares the same shape and has a delay of 1/6 time cycle because of the winding positions.

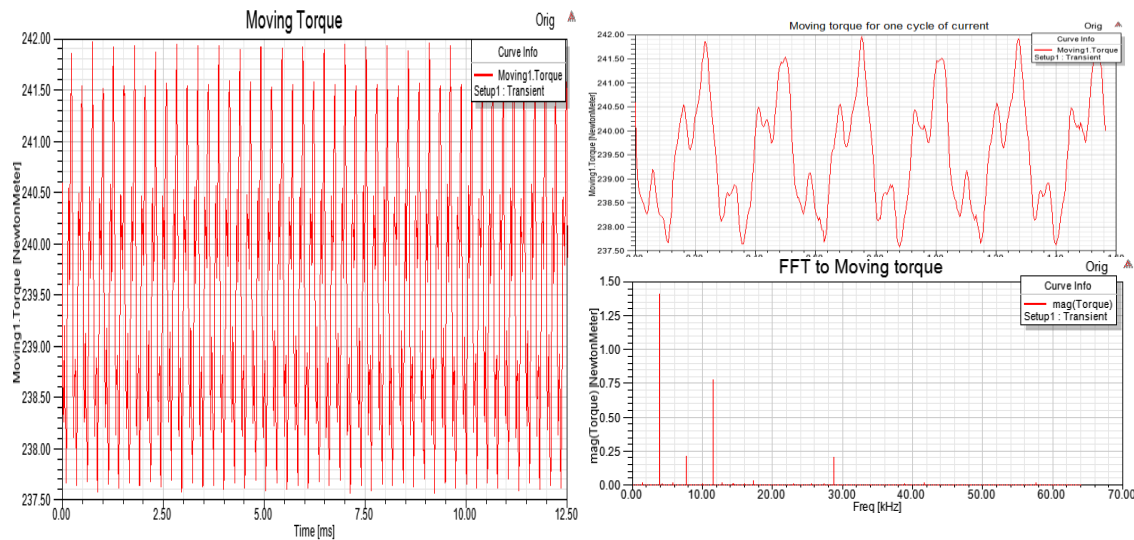


Figure 2.7 Moving torque and Fourier transform of torque

Moving torque of an electric motor is calculated as equation (2.20):

$$T = \frac{3}{2} p \cdot \vec{I}_s \times \vec{\Phi}_s \quad (2.20)$$

Here  $p$  represents the slot number,  $\vec{I}_s$  is the vector of input current and  $\vec{\Phi}_s$  is the magnetic flux vector. Choose moving torque of this model and apply FFT options for the magnitude of torque. Figure 2.7 illustrates the torque curve and Fourier Transform results. From this figure, torque curve has several fluctuations and the main time cycle for torque is 1/6 of input current. The main corresponding frequency of the fluctuation in FFT results is 3840Hz, 7680Hz and 10240Hz.

## 2.4 Parameters influence

Operating speed and power changing of the electric machine is achieved by controlling the input current. The three main parameters of alternating current are the amplitude, phase angle and electric frequency. Electric frequency mainly influences the rotating speed of rotor, while amplitude and phase angle affect the electromagnetic forces act on stator and rotor, while subsequently affect the operating torque and vibration behaviour. However, geometry changing mainly influences the radial and tangential force excitations which lead to the deformations as well as vibrations. Therefore, this section is mainly discussing the force variation under different parameters changing.

### 2.4.1 Amplitude and phase angle

Changing the amplitude (from 50A to 100A) and phase angle (between 90deg and 180deg) of input current in equation:  $I_s \cdot \sqrt{2} \cdot \sin(2\pi \cdot \text{efreq} \cdot t + \theta_A)$ , which is shown in table 2.1. The torque curve variation is shown in Figure 2.8.

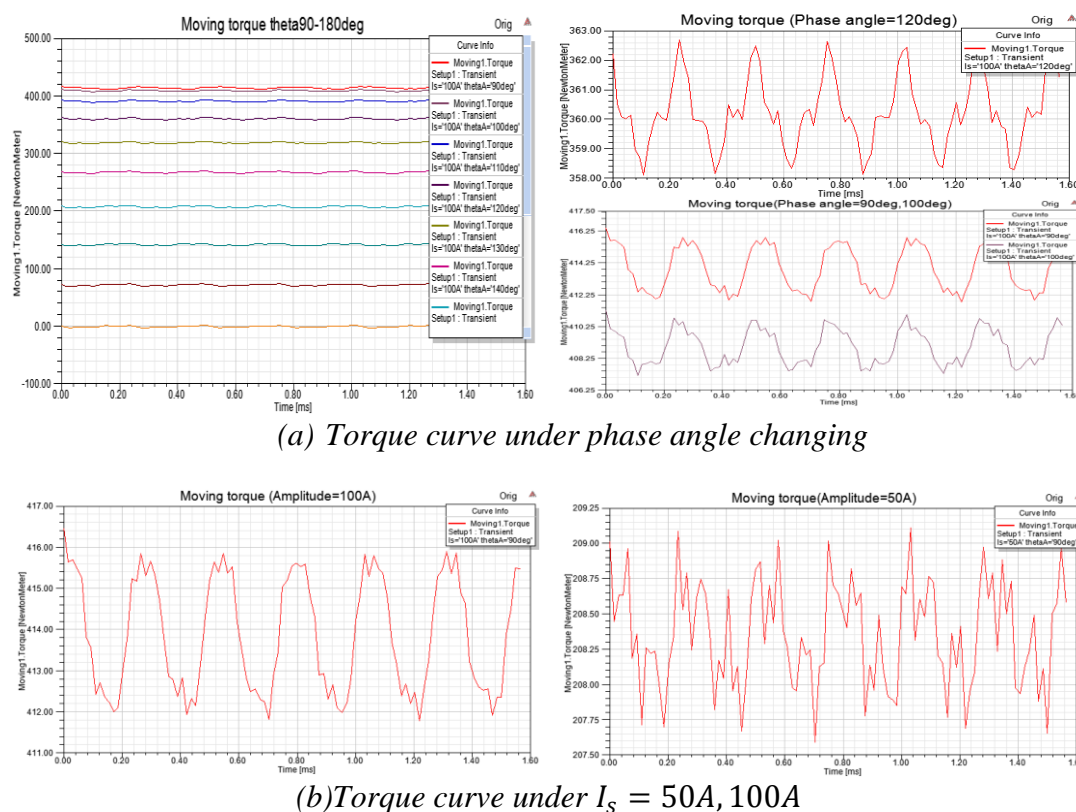


Figure 2.8 Torque variation

With the increasing of the phase angle from 90deg to 180deg the magnitude of moving torque decreases significantly, especially when phase angle equals the 180deg, torque value almost equals to zero. The difference of magnitude between every 10deg grows along with the phase angle's increasing, while the phase of every torque curve is delayed. Also the curve shape and the extra fluctuation frequencies are different. As shown in Figure 2.8(b), torque curve fluctuates significantly while  $I_s$  equals to 50A. The magnitude decreases along with the current amplitude. Hence, the operating condition of electrical machine is controlled by changing the electrical parameters. The electromagnetic force shares the same trends as load torque, but with small changes which shows in Figure 2.9.

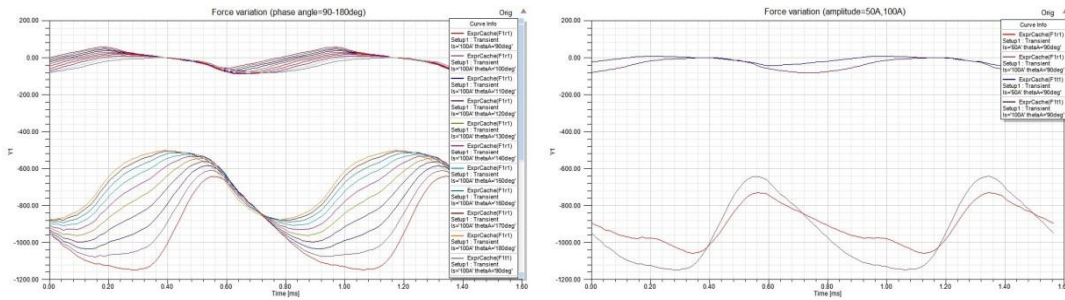


Figure 2.9 Electromagnetic edge force variation

## 2.4.2 Air gap size

Electromagnetic force of an electrical motor is produced due to the magnetic flux in the air gap, which means air gap length influences the flux density. Thus it influences the force significantly on the edge of stator tip and rotor. This will affect the operating performance and vibration response of a motor. The force results for changing air gap length as 0.2mm and 2.2mm is shown in Figure 2.10.

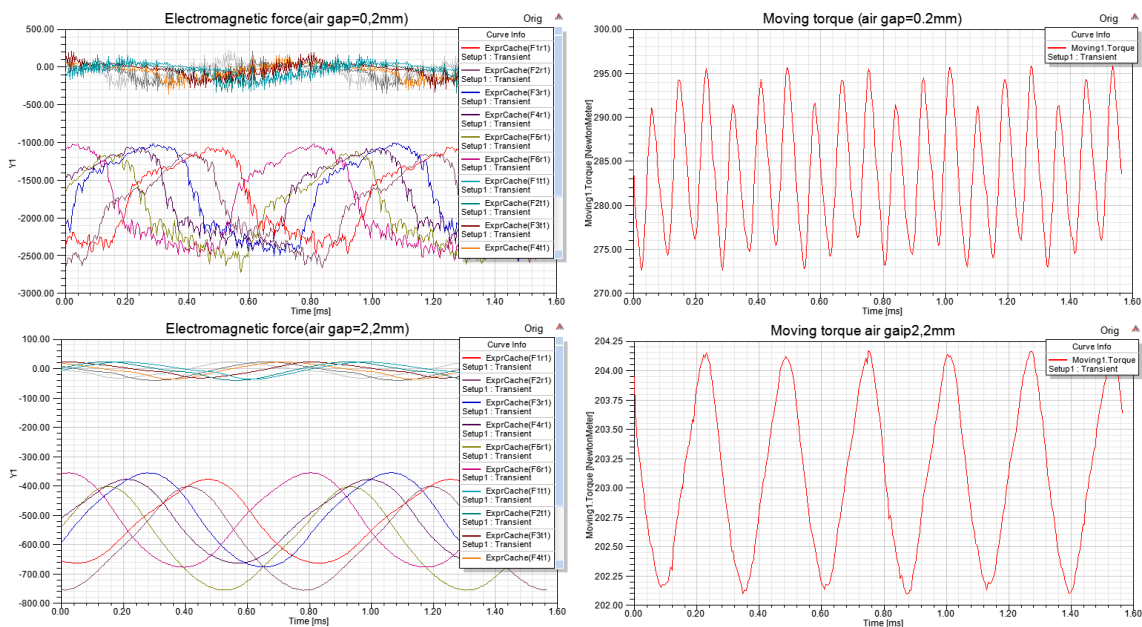


Figure 2.10 Moving torque and magnetic force under 0.2mm and 2.2mm air gap

Comparing the edge force illustrates in the above graphs, the absolute value of magnitude for 0.2mm air gap is much greater than for 2.2mm air gap, especially the radial component which causes vibration. The curve has many jagged waves and the value is extremely unstable since the flux density is high as well as interacts with each other in the small air gap. Moving torque is also fluctuated since it is generated from the tangential force acted on the magnets which is the opposite direction of the tangential part in Figure 2.10. For 0.2mm air gap, radial electromagnetic force is much greater than tangential one, while they are almost the same value for 2.2mm air gap. Therefore, by appropriate increasing the air gap, the harmonic force excitation can be reduced. Additionally, the curve can be smoother, thus the amplitude of vibration velocity can be reduced. However, a smaller air gap can improve the torque and power factor, but can produce the same size of rotating magnetic field with a smaller input current. Figure 2.11 shows the harmonic force excitation acted on the surface of stator tips of a 3D vibration model.

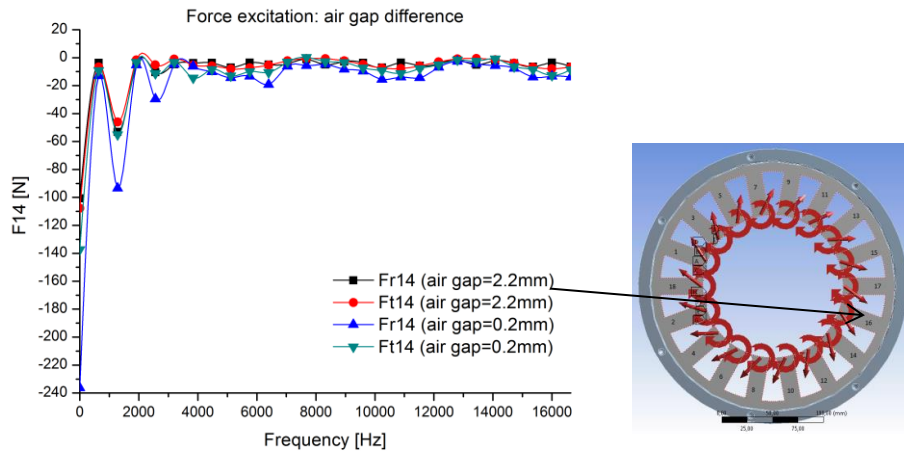


Figure 2.11 Electromagnetic force excitation (air gap= 0.2mm, 2.2mm)

### 2.4.3 Eccentricity

There are three groups of eccentricity: static eccentricity, which is often caused by the assembling tolerance; dynamic eccentricity produced by the uneven of the rotor mass, elliptical rotor surface and mixed eccentricity that is the combination of static and dynamic eccentricity. Rotor part is often off the center of the stator in static eccentricity, thus this causes the unbalanced distribution of the air gap which leads to the changing of magnetic flux. Here, Figure 2.12 illustrates a 50% eccentricity model in this simulation process. The rotor is closer to the positive direction of x axis than to negative direction.

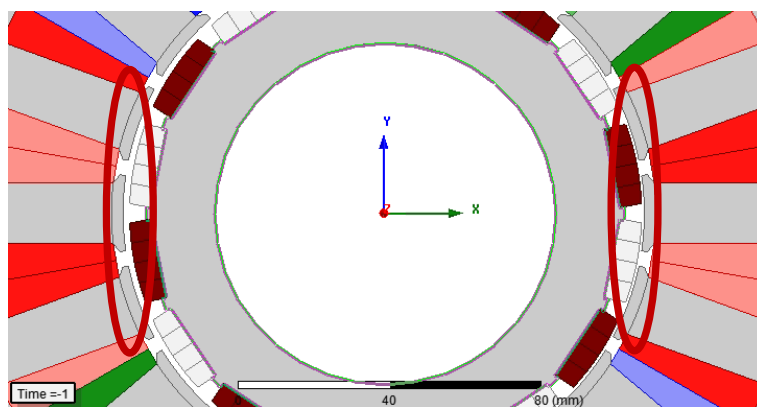


Figure 2.12 50% static eccentricity

Flux density in the narrow air gap is much higher than the other side which leads to the increasing of unilateral magnetic tensile force. It can be seen in Figure 2.13, amplitude of radial and tangential force along the narrow air gap grows nearly twice as the other side. Also this force curve is not a regularly sinusoidal wave. Besides, the tangential force is much less than the radial force. This will cause serious vibration but will not provide enough rotating torque to the rotor. In addition, moving torque becomes unbalanced for every time cycle, thus the torque curve is not a harmonic wave that means the electrical machine may not provide a stable torque output to the transmissions. Figure 2.13 shows the moving torque and force under 50% static eccentricity.

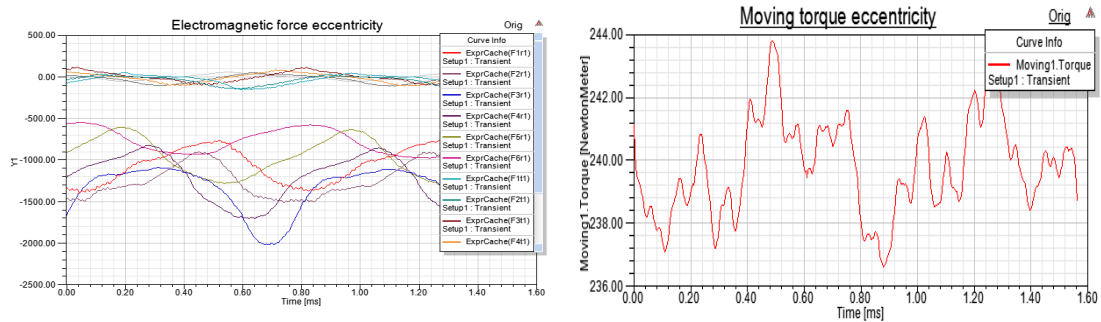


Figure 2.13 Moving torque and magnetic force under 50% static eccentricity

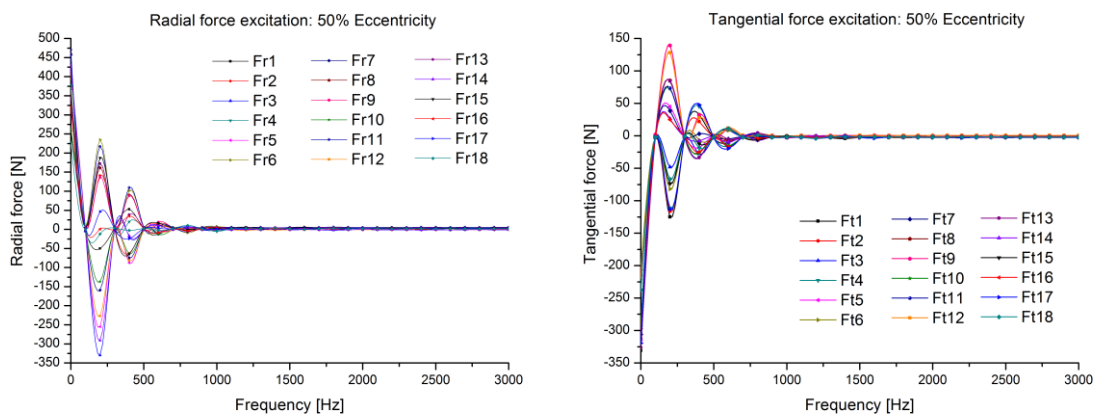


Figure 2.14 Force excitations on stator-tip surfaces

As can be seen from Figure 2.14, force excitations are centralized on the frequency range between 0 to 1000Hz and also the amplitude of radial vibration source grows greatly that is several times as tangential force, which means the vibration within this scale is dramatically increased. Besides, the serial number is defined from left to right that means number 1 to 9 is applied on the left part of the stator, while number 10 to 18 is defined in the opposite direction where the air gap is narrower. Therefore, the force excitation is fluctuated around 100N for the direction of large air gap, as it is around 300N to 500N on the side.

#### 2.4.4 Stator teeth thickness and tip width

Increasing the thickness of stator teeth, the absolute value of electromagnetic force excitation acted on the stator tips will decrease. This will make the reduction of the vibration amplitude and noise. Figure 2.15 shows the force excitation under different teeth thickness.

With the growth of tip gap (reduction of stator tip width), the edge length of stator tip decreases, then this will cause the diminution of force excitation, since harmonic force excitation equals to the integration of edge force density on tip edges. Figure 2.16 illustrates the harmonic excitation under different tip width.

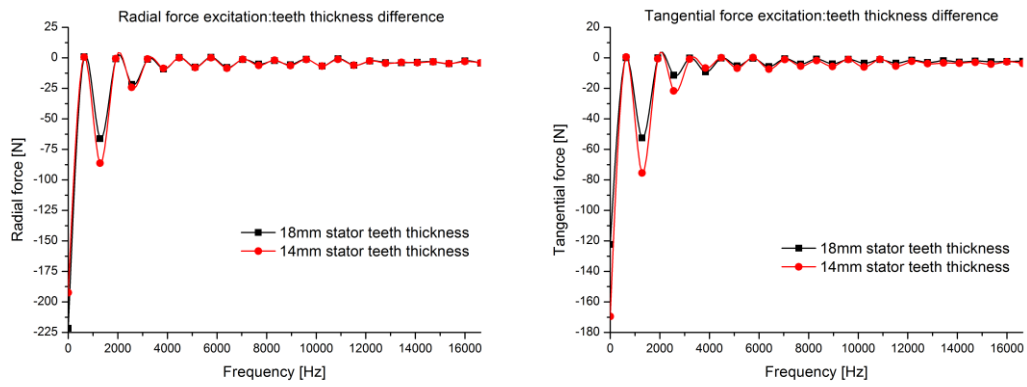


Figure 2.15 Electromagnetic force excitations under different teeth thickness

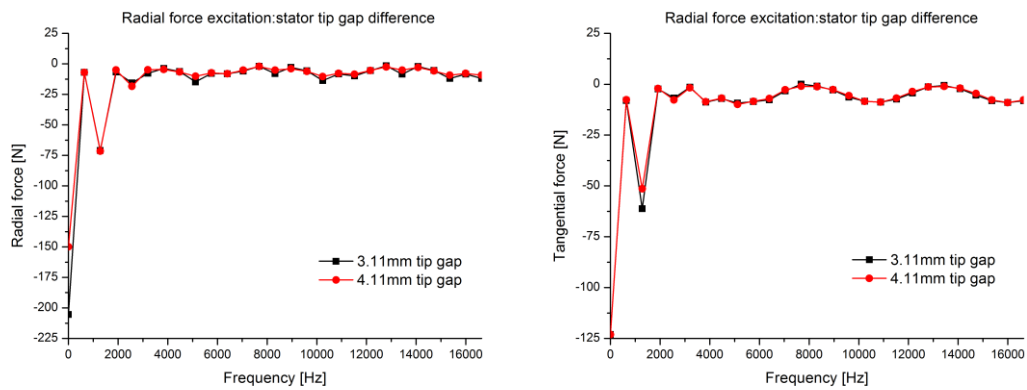


Figure 2.16 Electromagnetic force excitations under different tip gap

### 3 ANSYS Simulation Procedure

There are two important ways to calculate the vibration of one structure, analytical method and numerical method. Finite Element Method is used since analytical solution does not exist for arbitrary geometries. Therefore, FEA is used through the whole process of calculation. This chapter is focused on describing the simulation process using ANSYS Mechanical which is shown in the following Figure 3.1.

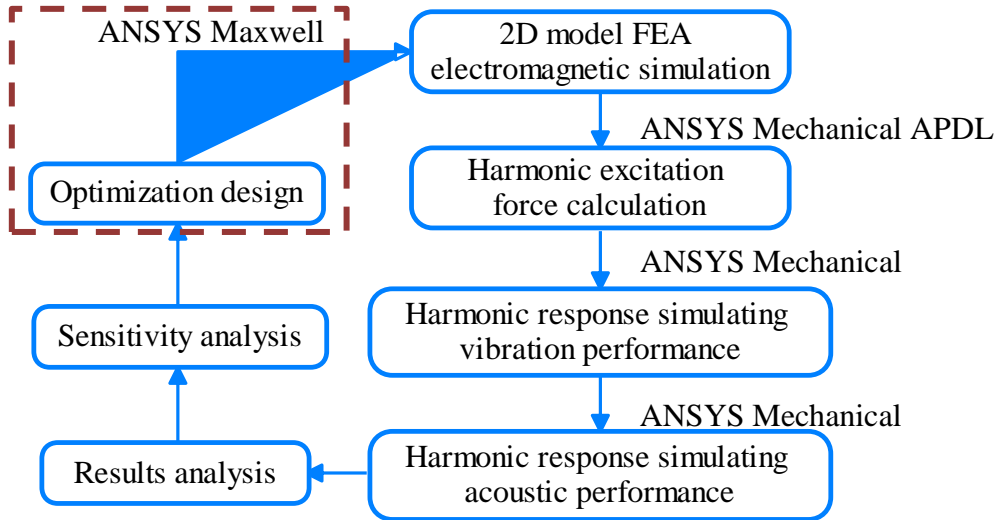


Figure 3.1 Flowchart of solution procedure

Use ANSYS Harmonic response solver to simulate the vibration of the electrical machine. The entire model is assumed to have constant stiffness and mass effects, moreover no transient effects are calculated. All the input and output loads as well as deformations vary sinusoidally at the same frequency which is known in the procedure. The whole system is presumed as a time-invariant and linear structure.

In a finite element method, all the displacement and deformation is calculated on every node of the meshes. Hence, the nonlinear vibration equation becomes:

$$[M]\{\ddot{x}(t)\} + [C]\{\dot{x}(t)\} + [K]\{x(t)\} = \{F(t)\} \quad (3.1)$$

Here,  $[M]$ ,  $[C]$ ,  $[K]$  is the mass, damping and stiffness characteristics respectively;  $\{x(t)\}$ ,  $\{\dot{x}(t)\}$ ,  $\{\ddot{x}(t)\}$  is the displacement vector, velocity vector and acceleration vector for every node; while  $\{F(t)\}$  is the load vector. ANSYS simulate one model using different time steps, thus full harmonic response analysis solves the system with simultaneous equations directly using sparse matrix solver and this solver is designed for the following equation:

$$(-\omega^2[M] + i\omega[C] + [K])(\{x_1\} + i\{x_2\}) = \{F_1\} + i\{F_2\} \quad (3.2)$$

where  $\{F(t)\} = (\{F_1\} + i\{F_2\})e^{i\omega t}$  represents a sinusoidal force excitation found by FFT and  $\{X(t)\} = (\{x_1\} + i\{x_2\})e^{i\omega t}$  is the sinusoidal displacement wave.

The two times derivations of displacement are shown in equation (3.3).

$$\begin{aligned} \{\dot{x}(t)\} &= i\omega(\{x_1\} + i\{x_2\})e^{i\omega t} \\ \{\ddot{x}(t)\} &= -\omega^2(\{x_1\} + i\{x_2\})e^{i\omega t} \end{aligned} \quad (3.3)$$

The advantage of the full harmonic method is easy to use and acceptable for all types of loads and supports. Moreover, no mass matrix approximation is involved.

### 3.1 Vibration analysis settings

#### 3.1.1 Material properties

Table 3.1 Part of material properties

Material	Components	Density (kg/m <sup>3</sup> )	Young's module (MPa)	Poisson's ratio
Structural steel	Stator simulated	7850	$2 \times 10^5$	0.3
M250-35A	Stator(real)	7650	$1.85 \times 10^5$	0.3
Copper	winding	8300	$1.1 \times 10^5$	0.34

Different material is used in this simulation and structural steel is used in stator instead of M250-35A.

#### 3.1.2 Mesh generation

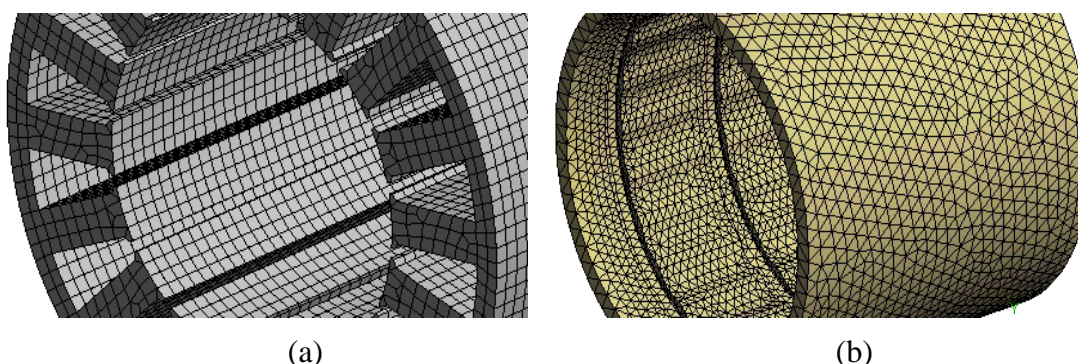


Figure 3.2 Mesh map

(a) Stator curvature mesh; (b) cooling cylinder patch conforming mesh

Choose physical preference of mesh property as 'Mechanical' to achieve the vibration mode shape. The relevance value is set between 0-20 to get the medium or slight fine mesh. Then the advanced global sizing function is defined as curvature which implies the mesh size is driven by the curvature encountered in the stator model. Since the stator model is dominated by many curved features, especially the force excitation is applied on the curved surface of start tip and windings. The stator meshing map is shown in figure 3.2 (a). Element size is defined in face sizing to control the elements number for the surface of the cylinder frame. A tetrahedral mesh is easier to generate but less accurate than a hexahedral mesh, so patch conforming mesh method is used to ensure a high quality surface mesh of the contact region between the stator and cooling cylinder. Figure 3.2(b) gives the cylinder meshes.

#### 3.1.3 Load and boundary conditions

The electromagnetic force load can be applied on the model using Fast Fourier Transform through ANSYS Mechanical APDL or directly imported the force

excitations from ANSYS Maxwell. Since this force calculation results are based on a 2D electrical machine model, remote force load should be added on the surfaces of stator tips. Figure 3.3 shows the remote force acting on stator tips and windings.

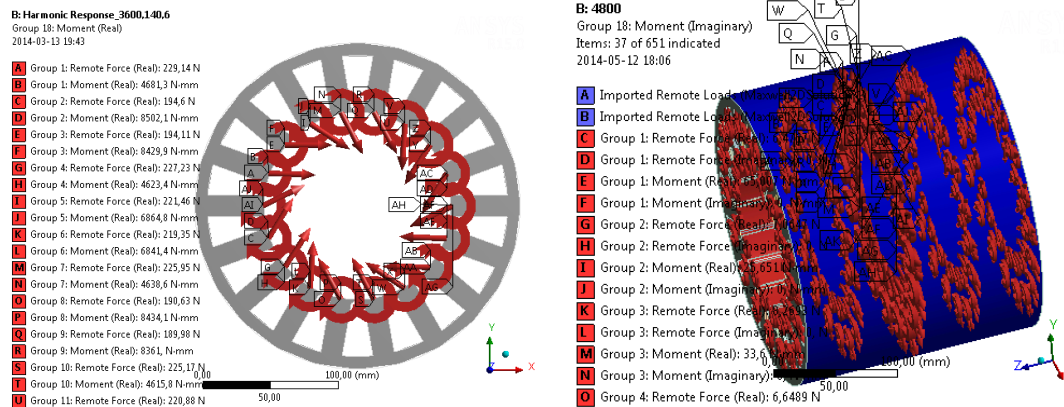


Figure 3.3 Load application

Fixed support is used on the six screw holes in the cooling cylinder. The screw connection is to connect the cooling system with the outer frame only in one end of the cylinder. Therefore, the vibration mode shape is different at opposite end.

### 3.1.4 Contacts

There are five types of contact behavior available in harmonic response solver. They are bonded type, no separation type, frictionless, frictional and rough type. The difference of behavior is shown in table 3.2.

Table 3.2 Behaviour of five contact types

Contact type	Separation	Sliding	Initially touching	Inside pinball region
Bonded	No gaps	No sliding	Bonded	Bonded
No separation	No gaps	Sliding allowed	No separation	No separation
Frictionless	Gaps allowed	Sliding allowed	Bonded	Free
Frictional	Gaps allowed	No sliding	No separation	Free
Rough	Gaps allowed	Sliding allowed	$\eta > 0$ , Bonded $\eta = 0$ , No Separation	Free

In manufacturing process, the stator is assembled with thermal expansion of the outer shell. After cooling procedure, stator has no separation and no sliding with the cooling system cylinder. Hence, bonded contact type is used to define this contact region. Alternatively define a whole part during geometry building in the simulation, since these two parts can be assumed as one body considered the contraction principle. For the winding model, the wires are wound around every stator tip. There are two contact regions for every wire model: one is the contact with the stator and another is with the neighbor wire. Gap between stator teeth surface and wires is not allowed

theoretically, but sliding along the radial direction of stator may be existed if it is not fixed in radial direction. However, there are always gaps between the wires under the condition of no filling materials. Hence, no separation and rough contact type is defined for the two contact regions in the simplified winding model. Assume wires are fixed in every direction, so bonded and no separation type is used in this simulation.

Here, for the cooling system cylinder, the fillings inside the tunnel is assumed as air when simulate the vibration mode shape of the structure.

## 3.2 Acoustic settings

Sound is a result of vibration and propagates in an elastic medium, like air, cooling oil. In this project, noise is generated by the vibration of electrical machine which is called a sound generator. When this structure oscillates, the air molecules around the stator surface vibrate and cause the vibration of the surrounding molecules. Thus this vibration spreads out as a sound wave in the form of longitudinal wave, the particle vibration is in the same direction with propagation of the sound wave and shear wave, where the direction is perpendicular with each other. The energy is transported from the transfer of particle momentum but not mass transfer.

Equation 3.4 is used to indicate the sound wave with small amplitude propagating in the ideal homogeneous medium.

$$\frac{\partial^2 p}{\partial x^2} + \frac{\partial^2 p}{\partial y^2} + \frac{\partial^2 p}{\partial z^2} = \frac{1}{c^2} \frac{\partial^2 p}{\partial t^2} \quad (3.4)$$

This equation can also be expressed as:

$$\nabla^2 p = \frac{1}{c^2} \frac{\partial^2 p}{\partial t^2} \quad (3.5)$$

Here,  $\nabla^2$  represents Laplace operator,  $p$  is the sound wave, and  $c$  is the sound velocity.

ACT extension solver is used to achieve the acoustic performance of the electrical machine by calculating the structure response at resonance frequencies. A sphere atmosphere around the model is simulated to get noise in the whole sphere air surrounding and it is sliced into six parts to gain the sound pressure level in the radial direction by suppressing the other four parts. The choice of the sphere radius is based on the experimental sensor position and the distance range which is most concerned. This body is defined as acoustic body and air is using as the medium of sound radiation. The mass density of air is  $1.2041 \text{ kg/m}^3$  and the sound speed is  $340 \text{ m/s}$ . Figure 3.4 displays the acoustic body.

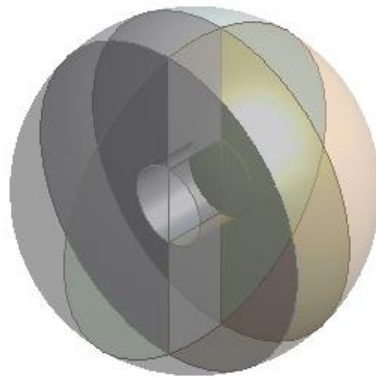


*Figure 3.4 Acoustic body*

Element size is defined in the sizing of acoustic and it concerns with the interest frequency range. This size should be less than a quarter of acoustic wavelength, where  $\text{wavelength} = \frac{340\text{m/s}}{\text{frequency}}$ . That is because the peak and trough value of every sound wave needs to be obtained when simulating the acoustic performance. Here, 340m/s is the speed of sound. The main concerned vibration frequency is within the range of 5000Hz. Hence, the body element size equals to  $\frac{340000}{5000 \times 4} = 17\text{mm}$ . Figure 3.5 gives the mesh map of acoustic body.

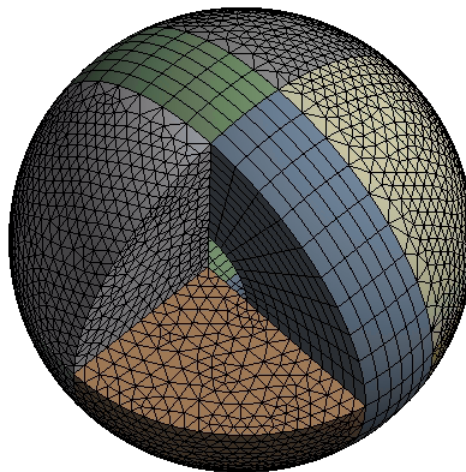


*Figure 3.5 Mesh map of acoustic body*

The boundary condition is defined by fluid structure interface. And robin condition (radiation boundary) is used to show the exterior is the natural boundary which is acoustics corresponds to a rigid wall.

## 4 Vibration and Acoustic Performance

Vibration source can be classified into three categories: mechanical, aerodynamic and electromagnetic force which is judged to be the most important force excitation caused the vibration of a PMSM. The force excitations act on stator tips, teeth and poles. Then it will transmit to the shells and chassis of the electrical machine. Therefore, the outer frame of stator also shares the vibration effect. However, these forces may be reduced because of the structure as well as the damping material inside the structure like the cooling oil or air inside the cooling cylinder. Damping is an energy-dissipation procedure which diminishes the vibration energy until stop. The influence for natural frequencies is small while damping is small. In this project, damping character is disregarded since damping of metal is small. However, this assumption will lead the inaccuracy in the winding model.

Every material has its own natural frequencies. In forced vibration, the external force excitation causes steady vibration response. When the frequency of excitation coincides with some of these frequencies, these vibration modes can be considerably magnified. This is mechanical resonance and these frequencies are resonance frequencies. Resonance usually occurs when a system is capable of storing and transferring energy between several different storage modes like electrical machine. Acoustic resonance is always relevant to mechanical resonance and is concerned with the vibrations across the audible frequency range of human, especially the unwanted sound: noise. The audible sound for human is normally the frequencies between 20 Hz and 20 kHz but responds more to frequencies between 500 Hz and 8 kHz which is the main concern frequency range in this paper.

Noise sources can be divided into four groups, magnetic, mechanical, aerodynamic and electronic. Magnetic source mainly comes from the slot harmonics and unbalance of the magnetic fields. Fluid cooling phenomena is counted in aerodynamic reason and switching harmonics belongs to the electronic source. While the most important source of noise is from mechanical vibration. This includes the vibration of stator, the balance and eccentricity of rotor. So, in this chapter, the vibration and acoustic performance of different structure model produced by electromagnetic force is simulated and analysed. Meanwhile, performance under different operating conditions is calculated here.

The simulation process is displayed in Figure 4.1 in ANSYS Workbench.

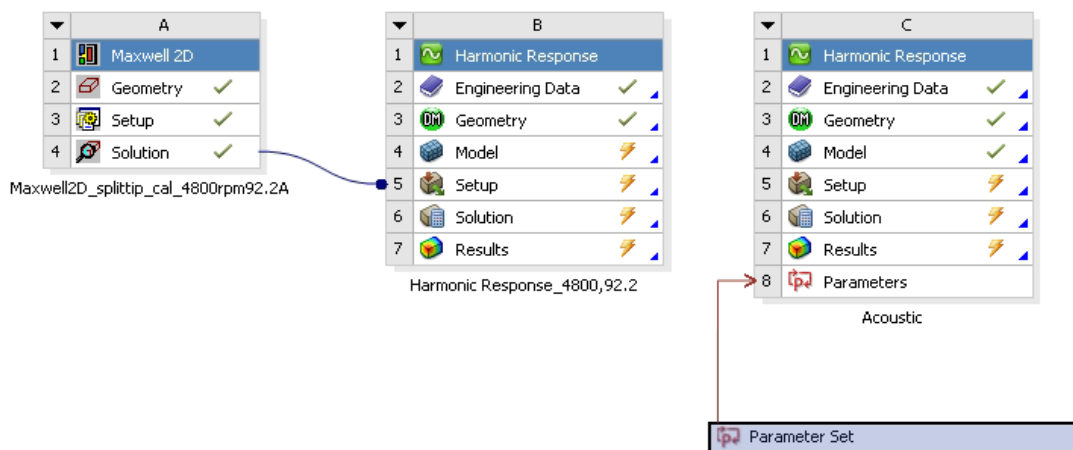


Figure 4.1 Simulation procedure in ANSYS Workbench

## 4.1 Stator vibration and noise

In this simulation, the operating speed of the electrical machine is 4800rpm and the load torque is 124.1Nm. At this time, the amplitude of the input current is 92.2A while the phase angle is 141.4deg. The calculation results in Maxwell 2D is a time domain result. After Fast Fourier Transform, the electromagnetic force excitation for every stator tip is imported. Figure 4.2 displays the force on the 14th stator tip. The force is mainly oscillated within 5000Hz. The frequency response of structure vibration from 0-16640Hz is shown in Figure 4.3.

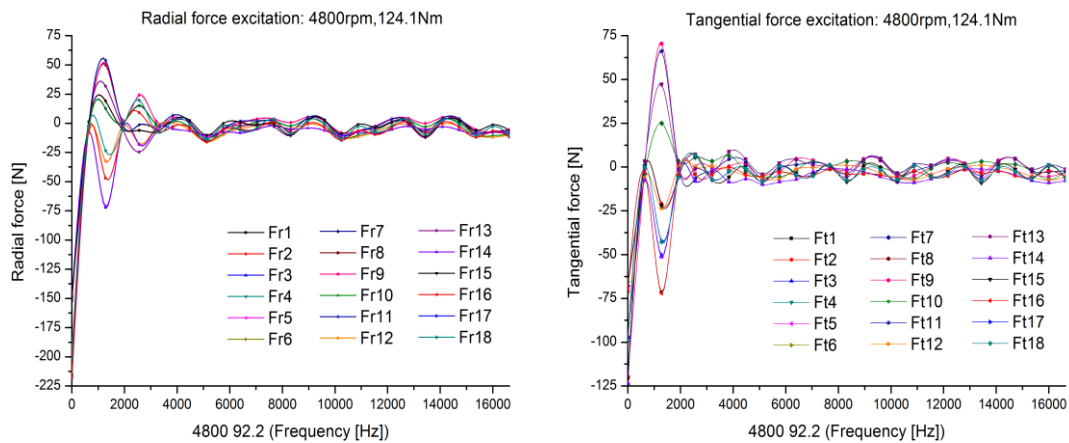


Figure 4.2 Electromagnetic force excitation in frequency domain

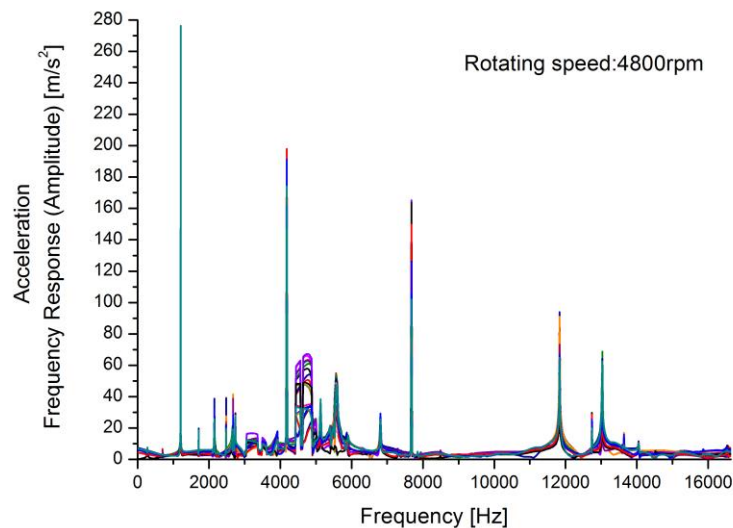


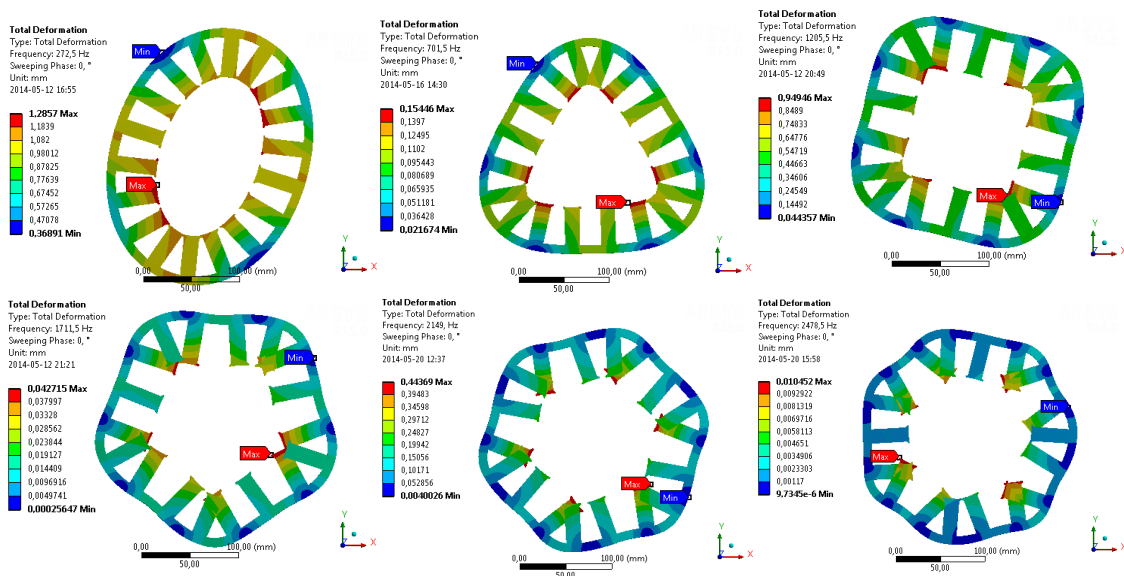
Figure 4.3 Frequency response of vibration acceleration on every tip

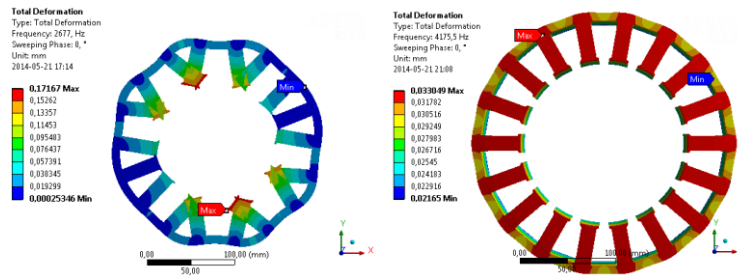
From the above picture, 0-5000Hz is the major vibration range of stator model, since the vibration acceleration curve oscillates severely within this range. And 1205.5Hz is the frequency with highest acceleration value. The top acceleration amplitude is about  $280\text{m/s}^2$ . Therefore, this simulation focuses on analysing the resonance frequency between 0 to 5000Hz. Moreover, the eight resonance frequency within 5000Hz is listed in Table 4.1.

Table 4.1 Resonance frequency for the first eight mode shape

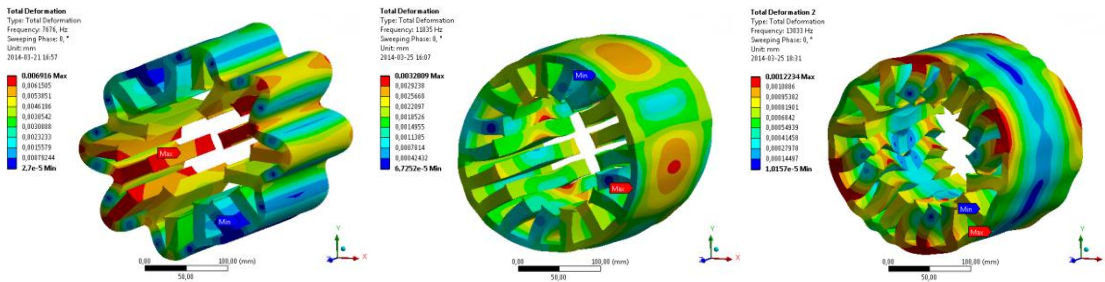
Mode shape	Resonance frequency(Hz)
1st	272.5
2nd	701.5
3rd	1205.5
4th	1711.5
5th	2149
6th	2478.5
7th	2677
8th	4175.5

There are three types of vibration, radial vibration which is generated by the radial electromagnetic force, axle vibration produced by the axle force and torsional vibration who is caused by torsional torque act on stator teeth. The first eight vibration mode shapes corresponding to every resonance frequency while the maximum deformation value is shown in Figure 4.4(a) which includes elliptical shape, polygons and expansion. These shapes are classified into radial vibration, because there are only two DOFs for every deformation shape. The vibration shape corresponding to high frequency is often irregular shown in Figure 4.4(b). Stator teeth deflect also in the tangential direction, meaning that tangential electromagnetic force has great effect on tangential deformation in high frequency range. Meanwhile, force excitation in high frequency is not always the same on every tip. Then the interaction between tips makes plane deformation shapes irregular and torsional. But the deflection value is quite small, so the main research frequency scale is still 0-5000Hz. The resonance frequencies are 7676, 11835Hz and 13033Hz respectively. Whereas, the mode shape and corresponding vibration response is shown in Appendix 2.





(a) Frequency range from 0 to 5000Hz



(b) Vibration in high frequency

Figure 4.4 Vibration mode shape (Total Deformation)

Acoustic response of the stator is simulated and Sound pressure level is the most concerned value. SPL, the abbreviation of sound pressure level, is a logarithmic measurement of the effective sound pressure value relative to the reference sound pressure value and it is shown in equation (4.1).

$$L_p = 10 \log \frac{p^2}{p_0^2} = 20 \log \frac{p}{p_0} \quad (4.1)$$

Here,  $p$  represents the effective sound pressure;  $p_0$  is the relevant sound pressure. It is defined as  $20 \mu\text{Pa}$  in air environment which is 1000times of audible sound pressure value. And the range of audible sound is from 0.5dB to 120dB. Sound will attenuate in the propagation process in air medium because of distance and air absorption characteristic. Among them, air absorption mainly influenced by temperature and humidity of environment is tiny. Therefore, it can be disregarded here while distance is the major affected factor. Then equation (4.2) illustrates the attenuation because of distance.

$$A_d = 20 \log \frac{r_2}{r_1} \quad (\text{dB}) \quad (4.2)$$

Here,  $r_1$  and  $r_2$  is the original and last distance relative to one vibration source.

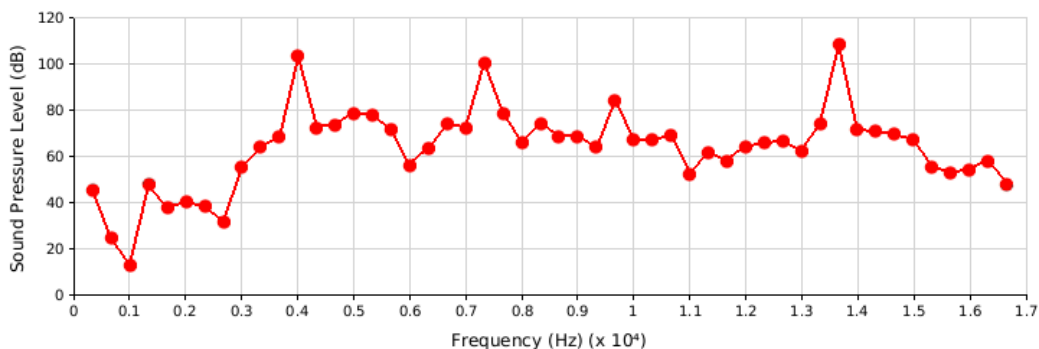


Figure 4.5 Sound Pressure Level for the stator center

Figure 4.5 illustrates the sound pressure level in frequency domain. This measure position is the center point of the stator and the highest sound is about 115dB which is very noisy to human. The corresponding frequency of the maximum SPL in Figure 4.5 is 4175.5Hz, 7676Hz and 13033Hz. However, with the increase of the distance from the vibration surface, the sound pressure will attenuate. And the acoustic performance within a radius of 0.5 meter sphere is shown in Figure 4.6. The highest SPL happens at the maximum deformation position of the vibration surface (stator surface) for every resonance frequency. For example, for 272.5Hz, peak sound value happens at the axle direction of the elliptical vibration shape. As can be seen in all the pictures, the sound waves also occur at the vertical direction to every peak sound wave. Furthermore, the sound pressure of radial direction is greater than of axle direction.

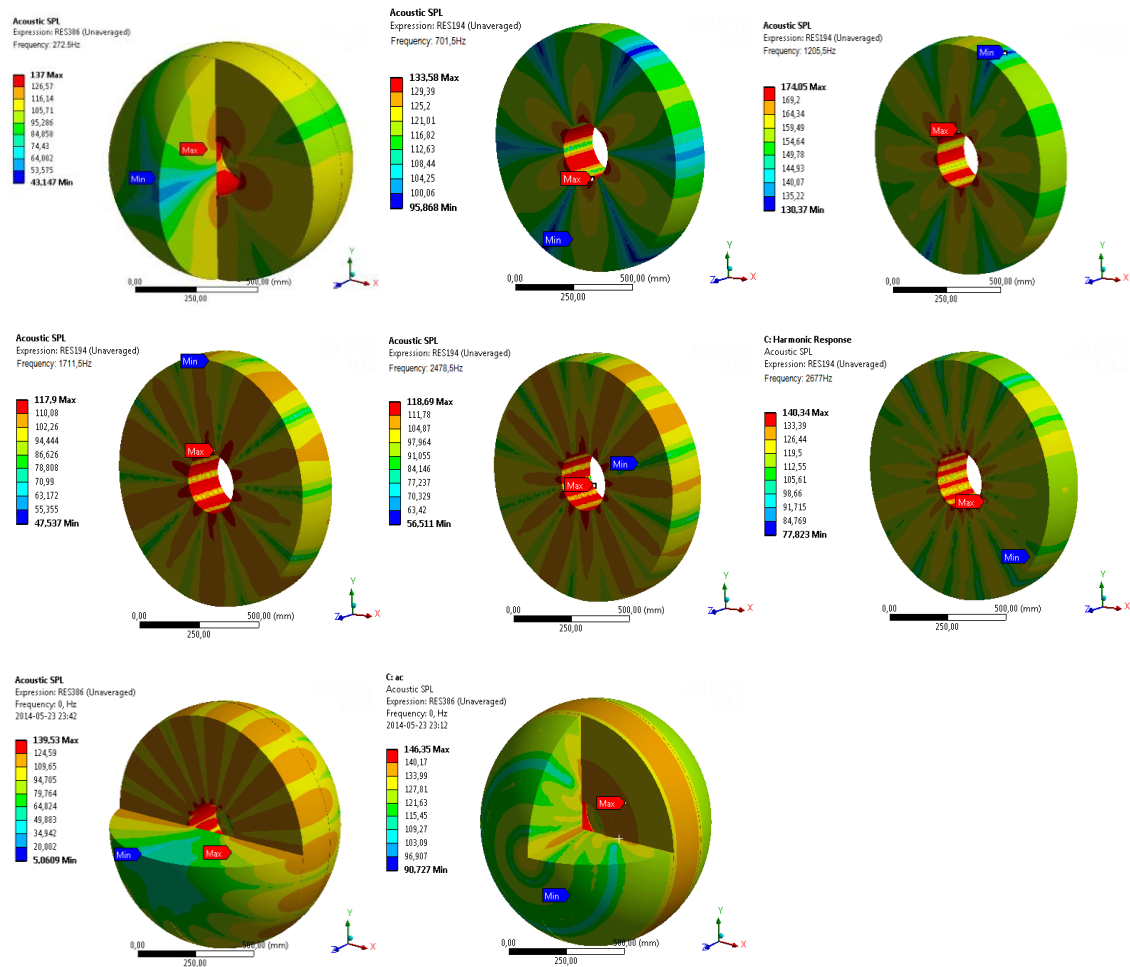


Figure 4.6 Acoustic contour plots within 0.5m radius

Consider that the stiffness of stator lamination is less than of an entity body and the natural frequency for M250-35A is also less than for structural steel, the corresponding resonance frequency for every mode shape decreases by around 8-12%. (Tianyu WANG, Fengxiang WANG,2007) Due to the relatively high damping, lamination structure may reduce the vibration mode response. However, a torsional vibration exists because of the friction between every layer. But this lamination impact on vibration is less compared with other structures; therefore, the stator model with solid structure steel is still used in the simulation in next step.

## 4.2 Influence of operating points

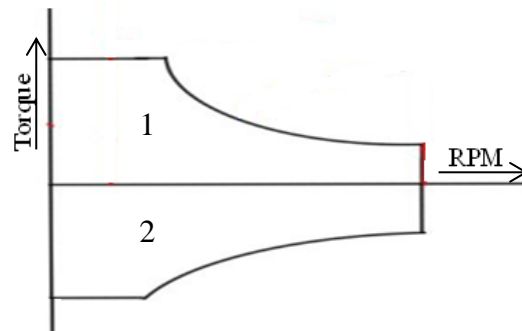


Figure 4.7 Torque curve of electrical machine

Figure 4.7 is a torque curve of electrical machine. In a hybrid vehicle control unit, electrical machine is used as a generator to generate electricity and as motor to provide power to vehicles. Under curve 1, machine transfers electric energy into mechanical energy as a pure electric motor. The area of curve 2 is a regeneration mode when the machine works as a generator to provide electric energy stored in the battery. Table 4.2 indicates the operating points of this machine within curve 1 and x axis which are calculated and analysed in this section.

Table 4.2 Operating points of high rotating speed

Speed(rpm)	3600		4800		6000	
Torque(Nm)	166,3	196,5	124,1	146,6	99,2	117,2
Power(kw)	62,7	74,1	62,4	73,7	62,3	73,6
Amplitude(A)	97,7	140,6	92,2	127,0	91,7	120,6
Phase angle(deg)	128,2	139,3	141,4	147,4	149,7	153,2

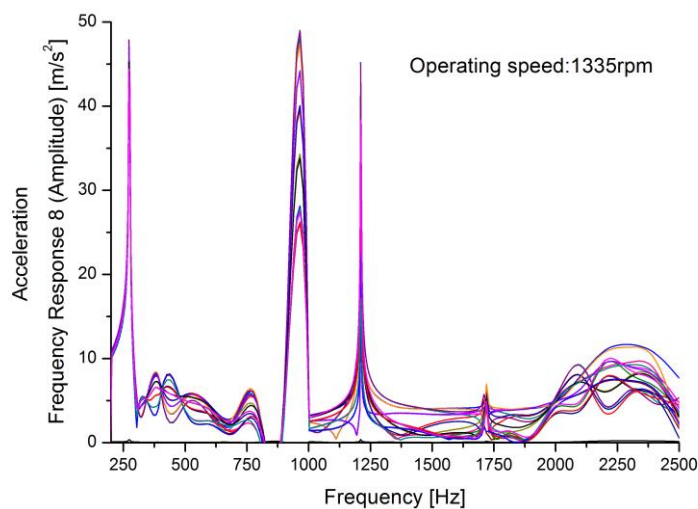


Figure 4.8 Frequency response under 1335rpm on every tip

The demands on electrical motors for HEVs differ greatly from those on traditional industrial motors, especially when it comes to power density. However, pushing torque and speed towards the limit also means that noise and vibrations will increase. When machine works at low speeds, the vibration acceleration and deformation is both lower than in high speed. Also the vibration frequency range is small which means the plane mode shape is limited. Therefore vibration performance under a high rotating speed is worth researching. Here, the frequency response under 1335rpm is shown in Figure 4.8.

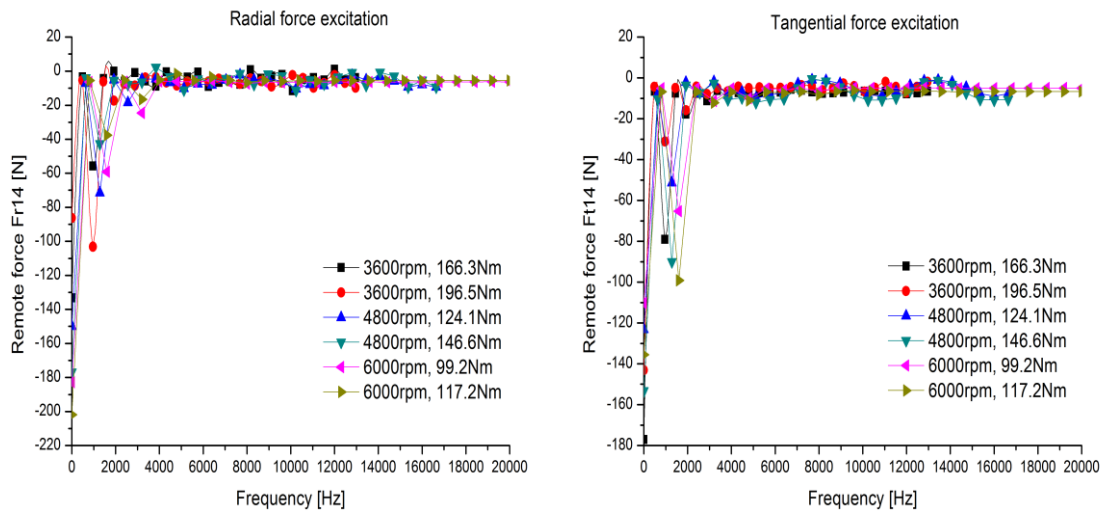


Figure 4.9 Radial force excitation acted on the 14th stator tip

As shown in Figure 4.9, the radial magnetic force excitation grows with the increasing of the rotating speed. Furthermore, the amplitude of tangential force is higher than of radial one. But radial force excitation rises faster and becomes much higher than tangential one as the operating speed is increasing, which means that vibration response will be greater when improve the speed and torque requirement of the electrical machine in Hybrid-electric vehicles. However, the corresponding frequency for force waves shown in x axis keeps constant at different operating speed. These excitations are all centralized within 0-5000Hz, especially in the range of the first three radial vibration mode. Figure 4.10 expresses the frequency response of vibration acceleration.

The resonance frequency and mode shape remains the same when changing operating points. However, the deformation amplitude is different, thus the maximum deformation for one tip is 1.27mm on 272.5Hz when it works at 4800rpm which is indicated in Figure 4.11. It can also be seen from Figure 4.10, the frequency response for vibration acceleration has peak value as  $280\text{m/s}^2$ . The corresponding frequency is around 1300Hz at 4800rpm. Compare the vibration performance under different speeds, 4800rpm owns the maximum acceleration amplitude and deformation value, since the electric frequency 640Hz is a disturbance frequency which can make natural frequency amplified. In addition, around 1200Hz is the region with high vibration response.

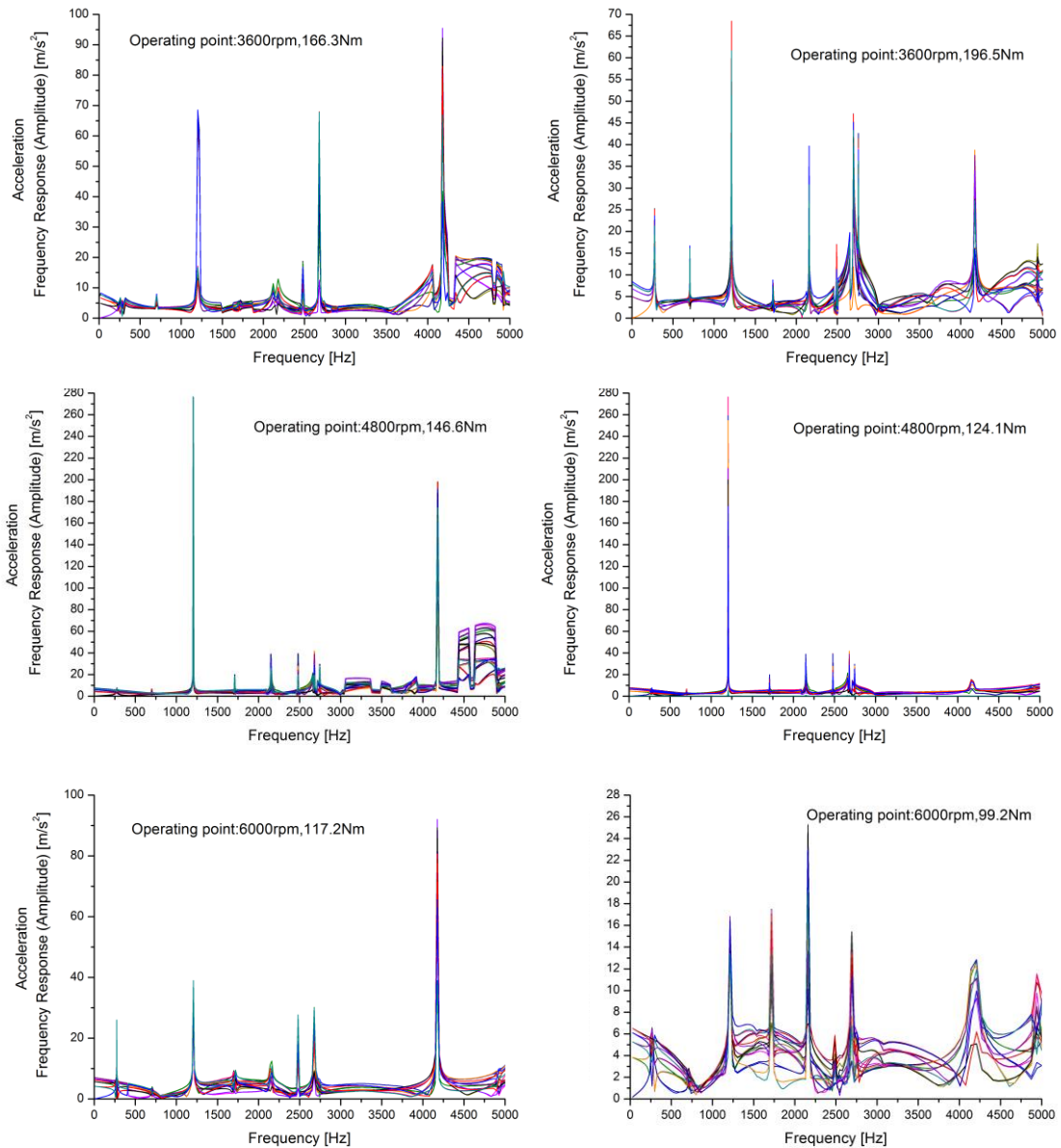


Figure 4.10 Frequency response under 6 operating points

When electric machine works at 6000rpm (the highest rotating speed of this simulated motor), the mode shape at high frequency is torsion and shear vibration, like in 13644Hz, 18200Hz and 19952Hz shown in Figure 4.12. Antisymmetric vibration mode appears at the two ends of stator, though the amplitude of deformation is small. That is because the magnitude of tangential electromagnetic force is greater than of radial one in high frequency range.

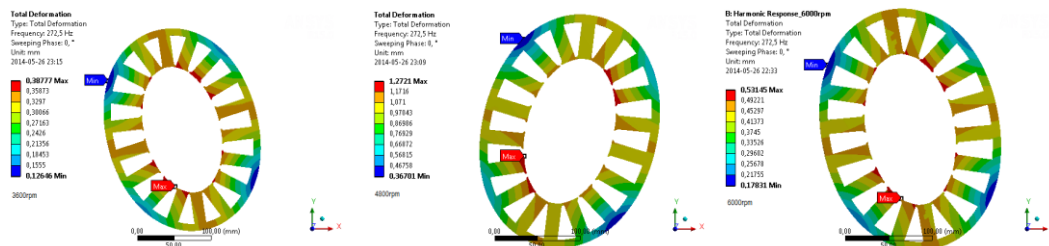


Figure 4.11 Stator deformations under different speeds at 272.5Hz

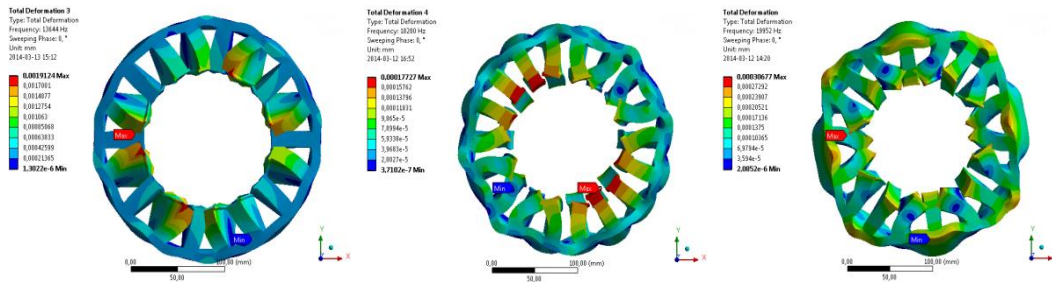


Figure 4.12 Mode shape in high frequency at 6000rpm

The average level of sound pressure in 4800rpm is the highest which is 120dB in around 1200Hz. And then SPL in 6000rpm is higher than in 3600rpm. Apparently the noisiest sound is for every speed is in the resonance frequency range. Hence, optimal design for acoustic is to reduce the SPL, at the same time increase the homologous frequency.

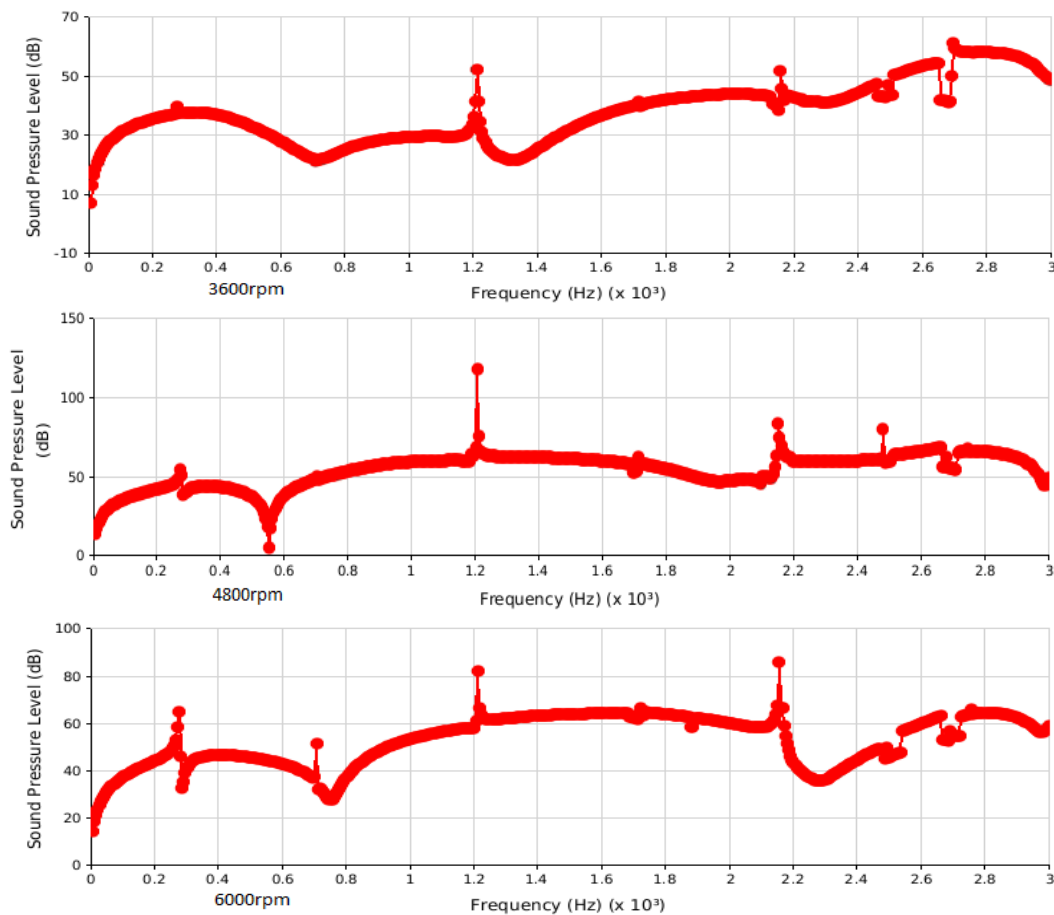


Figure 4.12 Acoustic performances under different speeds

### 4.3 Structure influence

The main components of an electrical machine are stator, rotor, windings and frame. However, vibration of rotor is caused mainly by the inertia because of the high rotating speed, but not electromagnetic force. Therefore, rotor does not influence the stator vibration performance except for the eccentricity of rotor assembling or manufacturing deviation. Electromagnetic force excitation acted on stator tips remains the same when outer structure is added. Yet the weight, material, contact area of the

other component has great impacts on the vibration frequency. Here, since the cooling system cylinder directly contacts with the stator surface, it is the major concerned outer part. In addition, slots and static eccentricity impacts are discussed in this section, too.

### 4.3.1 Cooling system shell

In this section, vibration and acoustic performance of two shell model is simulated. One is a simple cylinder with fixed support and the other is a real cooling system frame using in the EM prototype with cooling tunnel. Also model with different length of screw hole is simulated to estimate the influence on vibration response of fixed support parameters.

#### 4.3.1.1 Simple shell

This is an exterior cylinder structure with 6 screw holes as fixed support connected with the outer frame of the electrical machine. The inner cooling tunnels are disregarded to check the influence of the contact area. The mass of this model is heavier than the complex shell because of the filling steel in these tunnels. But contact area is the main affected factor.

*Table 4.3 Natural frequency for the mode shape within 0-5000Hz*

Mode shape	Resonance frequency(Hz)
1st	998
2nd	2200
3rd	2961
4th	3880
5th	4200
6th	4380
7th	4760

Inside the range of 0 to 5000Hz, only the first 7<sup>th</sup> mode shape exists. Owing to the outer cylinder, the frequency corresponding to the every mode shape increases by hundred to thousand Hz and the amplitude of acceleration reduces by nearly 20% when compared with the vibration model of the pure stator, seen in Figure 4.13. For example, natural frequency for the first elliptical mode shape enhances from 272.5Hz to 998Hz.

$$\omega_n = \sqrt{\frac{k}{m}} \quad (4.3)$$

In equation (4.3),  $\omega_n$  is the natural frequency of the system which is mainly decided by stiffness and mass of the structure. Here, the fixed support for screw holes increases the system stiffness dramatically, while mass also grows. However the increasing of mass is much less of stiffness. Therefore the resonance frequency of this model is finally increased.

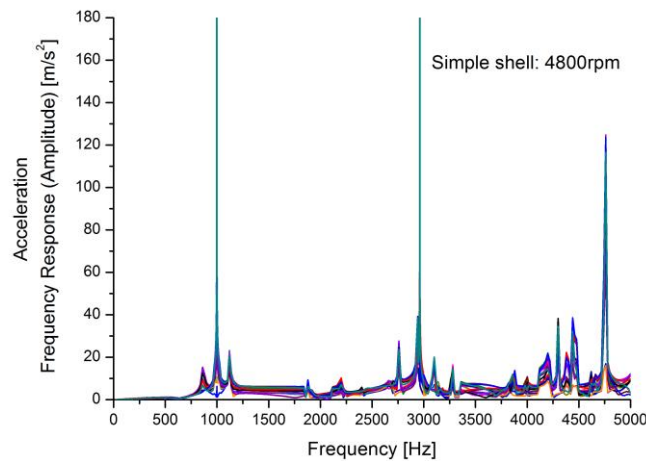


Figure 4.13 Frequency response of simple shell model

Since the fixed support is added on one end of the stator and the screw holes do not go through the whole stator, the deformation in this side is limited and the deflection on the screw point equals to zero. Still the deformation amplitude is large on the opposite end of the stator because of no restriction of movement in radial direction. But with the increasing of the frequency, the mode shape in the two ends of z axis is almost same, that means the vibration amplitude is weakened. There is slight shear vibration in high frequency. Figure 4.14 shows the deformation responding to several resonance frequencies.

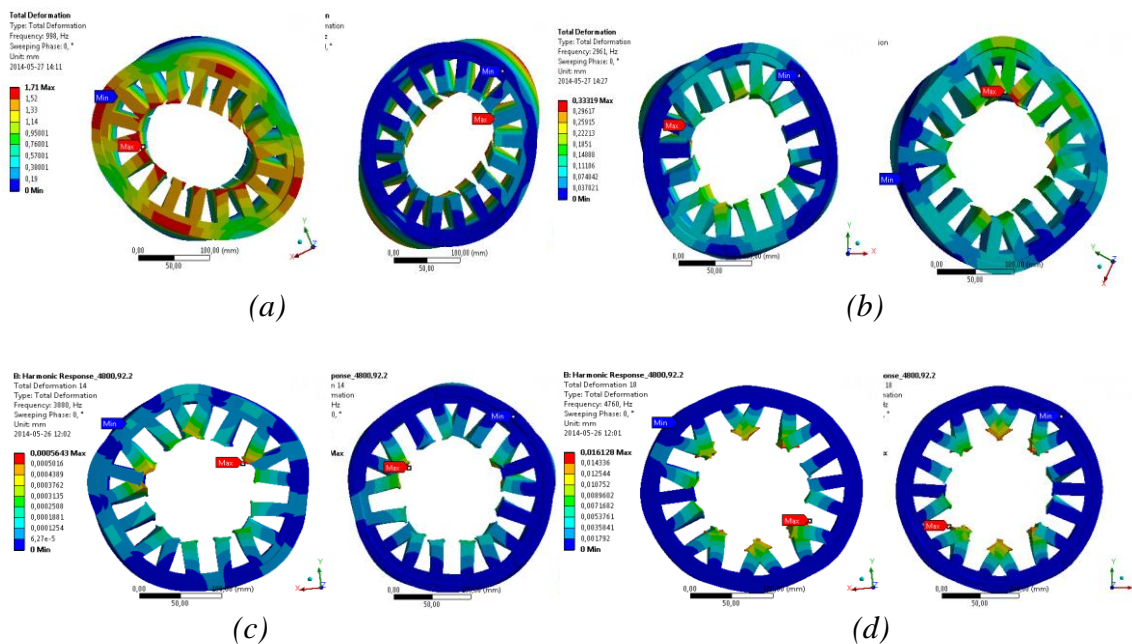


Figure 4.14 Deformation response

(a) 998Hz; (b)2961Hz; (c)3880Hz; (d) 4380Hz;

Extend the six screw holes to get through the whole stator in z direction, the free deformation of stator is limited and acceleration amplitude is dramatically decreased. As is shown in Figure 4.15, the maximum deformation for every mode is reduced, especially for the first three mode shapes. These vibration responses are diminished and do not appear as elliptical, triangular and square shape. However, the other

vibration mode shapes within 5000Hz still exist. Furthermore, the corresponding frequency for the other modes increases since the stiffness of system improves and the mass decreases. Therefore the extension of the fix support length affects both resonance frequency and vibration response which means the vibration and acoustic performance can be improved by extend the fix holes. Figure 4.15 shows some vibration response of this model.

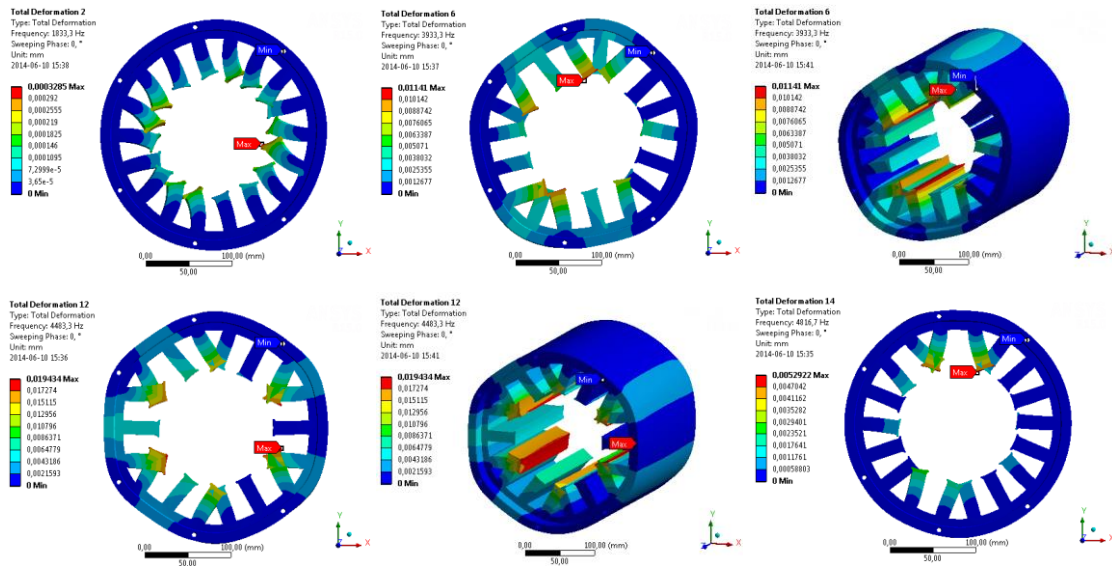


Figure 4.15 Vibration response

### 4.3.1.2 Complex shell

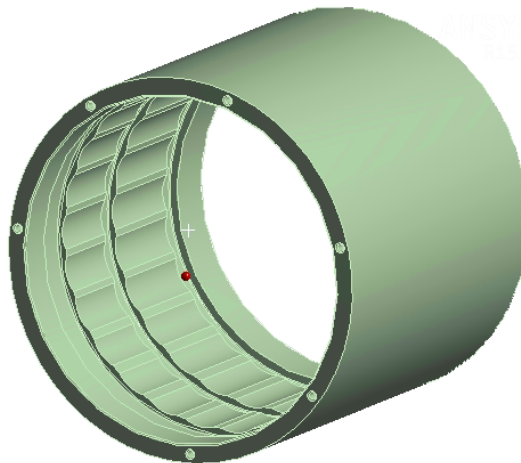


Figure 4.16 Cooling system shell structure

This complex shell is the one used in the real electrical motor with tunnels filled of cooling oil. The contact region is small and contact area for every tunnel is in different size. In the test machine, the exterior cover contains several holes to drain the cooling oil and the edge fillet which is both ignored in the simulation model because the elements for patch conforming meshes will dramatically grow and the most concerned influence factor is the contact region in this simulation. The structure of exterior frame is shown in Figure 4.9.

Table 4.4 Natural frequency for mode shapes within 0-5000Hz

Mode shape	Resonance frequency(Hz)
1st	845
2nd	1805
3rd	2780
4th	3050
5th	3830
6th	3995
7th	4115
8th	4970

Both resonance frequency and deformation in this model is less than in simple shell model owing mainly to the contact area changes. As the contact area between cooling cover and stator exterior surface decreases, the stiffness of the whole system diminishes. The whole mass of this system also shrinks, but is less than stiffness reduction. With the application of damping material inside the tunnel, the vibration amplitude is reduced, as well as the corresponding frequency. Here, substance in the tunnel is default as air. Hence, both deformation magnitude and resonances reduce in this simulation model. Figure 4.17 shows the mode shape of complex model.

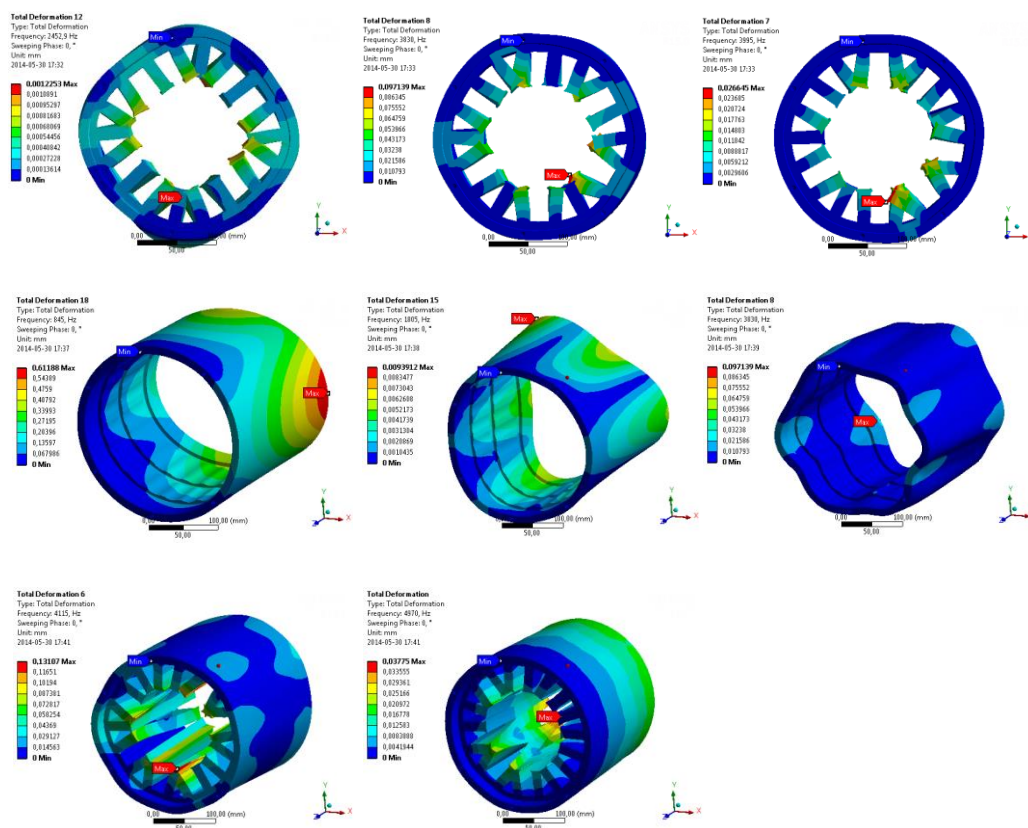
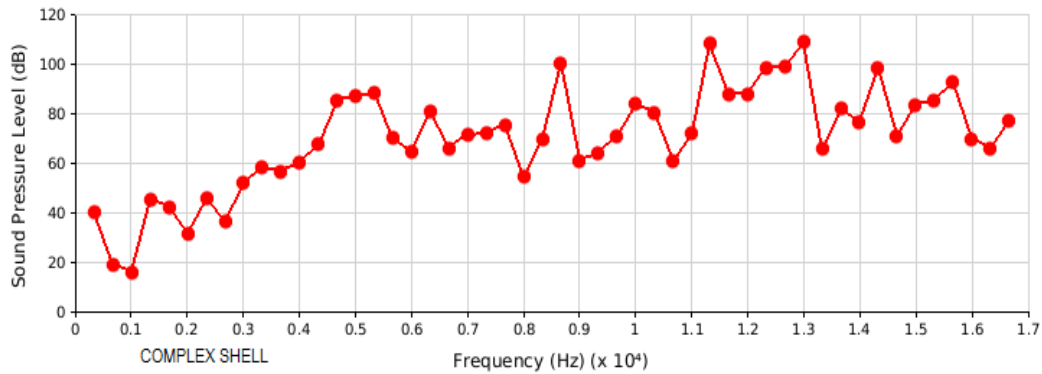
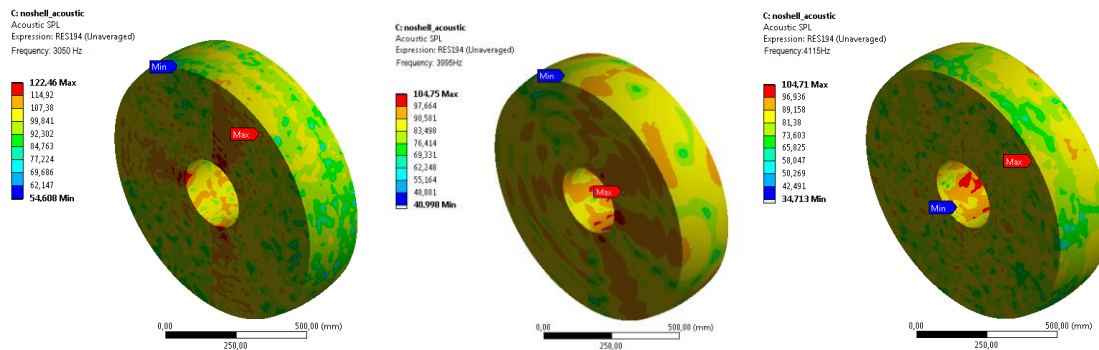


Figure 4.17 Vibration mode shape of complex cooling shell

In this model, the interface between structure and air is the exterior cover of cooling cylinder. It can be seen from the above contour plots, the deformation energy transferring from stator tips to exterior cover is diminished. And the propagation wave of sound is not regular because of the irregular vibration of the frame with six fixing points. Hence, acoustic performance shares the same tendency with vibration response and is less than in pure stator model.



(a) Sound pressure level



(b) Contour plots for SPL within 1m atmosphere

Figure 4.18 Acoustic performance of complex shell

### 4.3.2 Windings

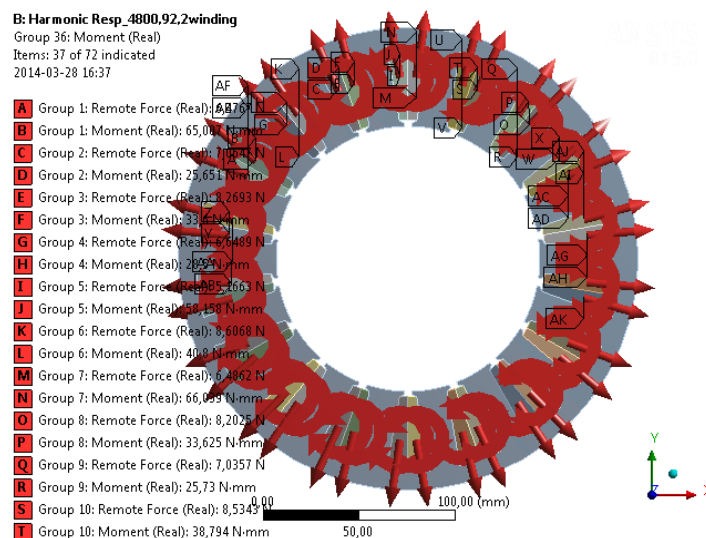


Figure 4.19 Slots force excitation

Here, winding part is assumed as a solid volume with the material of copper and the weight of the end part is disregarded. The plastic material wrapped with the copper line is also ignored, but this will influence much to the final results. In this model, force excitation acted on the 36 windings is applied (Figure 4.19), though pressure on stator tips is still the main vibration source. Since the tips' area is much bigger than windings.

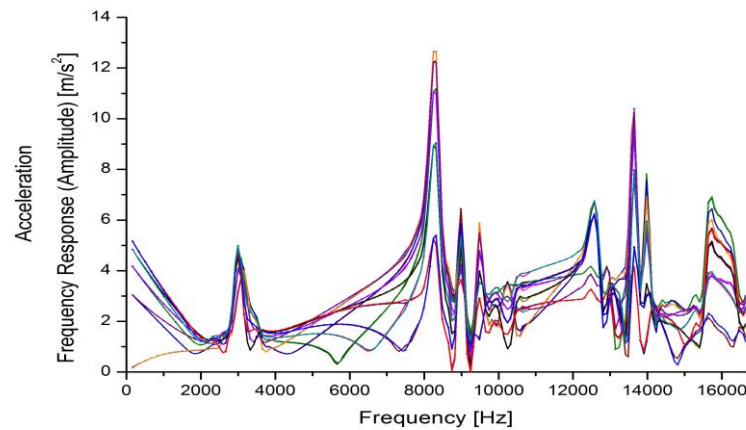


Figure 4.20 Frequency response of slots model

As shown in Figure 20, the corresponding frequency of elliptical mode shape is 2995.2Hz which is much greater than pure stator model and shell model as well as the other resonance. Moreover, it does not coincide with the experimental resonance. It is mostly because the assumption of the material and shape of the slots model. The winding volume filling with copper has a heavier weight than the real coils. Moreover, the stiffness of rubber is much less than of metal material. Here, the equation of natural frequency is  $\omega_n = \sqrt{\frac{k}{m}}$ . Then the weight increasing and relatively higher stiffness improvement makes the natural frequency of simulation model far bigger than the real model.

One way to solve this problem is to replace the slots model with both poly and copper layer. This method is used to enhance the calculation accuracy from structure aspect. However, it will add new issues, like the contacts between two layers and a simulation complexity. So this is not an effective method in this simulation.

The other way is to utilize a new homogeneous compound material taking place of copper and poly. Additionally, density and stiffness can be recalculated according to the capacity. This way is called equivalent material method. This new material may not be a real substance, but is a material with new density and stiffness as Young's Module and Poisson's ratio.

The third way to resolve the inaccuracy simplified model is making the slots an attached mass on the stator tip. Meanwhile, the force excitation on windings is integrated into forces on tips.

Last but not least, use a dynamic elastic modulus to replace the static one, since the elastic modulus is not static when copper line is wrapped on the tips. Here, a dynamic elastic modulus equals to the multiplication by an attenuation coefficient and the static elastic modulus. Nevertheless, the attenuation coefficient is not linear, thus it should be recorded in the real test with a winding stick.

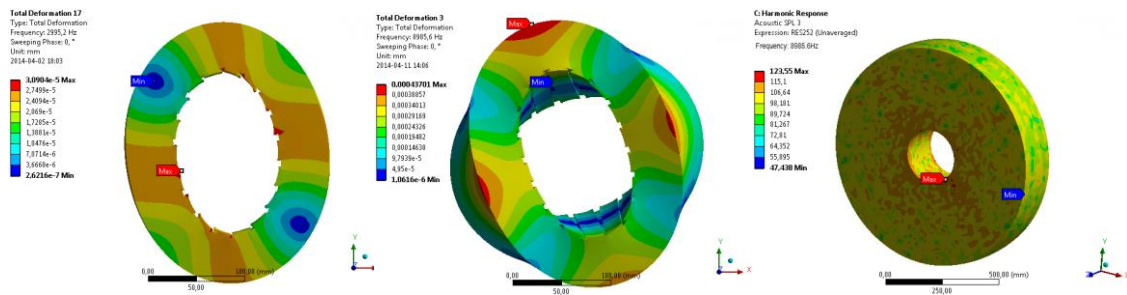


Figure 4.21 Vibration and acoustic performance

## 4.4 Rotor eccentricity

Rotor eccentricity causes an extremely high frequency response of deformation even reaches as an average value of 33mm for the maximum deflection in first mode shape of ellipse in 272.5Hz. This is owing to the high radial electromagnetic force growing which is mentioned in Chapter 2. When considering the fixed support points, an asymmetric vibration mode appears in radial direction (XY plane) especially in x direction which is owing to the unbalanced distribution of force excitation. Since the rotor is 50% eccentricity in x axis with stator center.

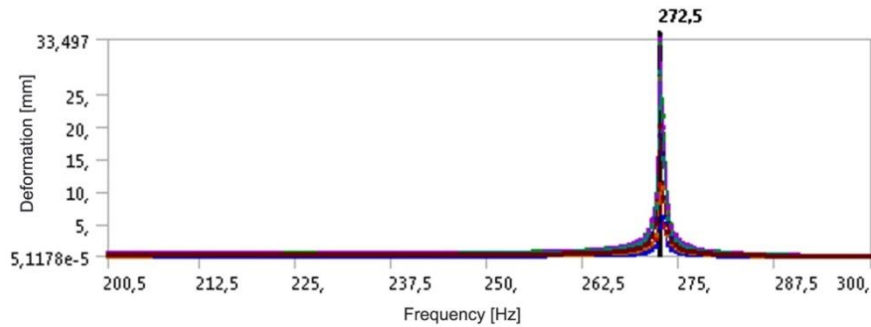


Figure 4.22 Frequency response of deformation

## 4.5 Experimental results

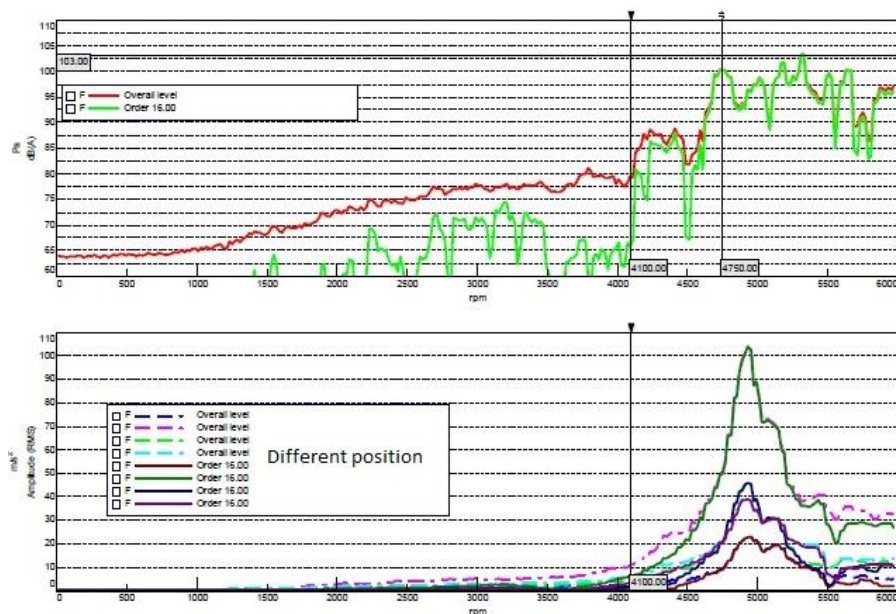


Figure 4.23 Sound pressure and vibration in one test

Experiments on a prototype vehicle with freely rotating wheels were done in the lab. The motor is attached to the vehicle and the gear box. A motor speed sweep has been performed, from zero speed to 6000 rpm with 20rpm steps. A microphone and accelerator meters were used to record the sound pressure and vibration acceleration. The microphone is positioned about 1 meter from the vehicle. Here, only the results that motor is separated from combustion engine are recorded.

Though the force excitation is not only electromagnetic, the frequency response still can be used to compare with the stator and frame simulation. Since the pattern of the excitation is different: electromagnetic forces are always harmonic waves as long as the input current is a sine wave and are the most important vibration source, but mechanical forces may be transient waves or linear curves. The test results showed that the gear sounds are very low compared to the one from the electric motor. There are only smaller changes in the sound during operations at different gears.

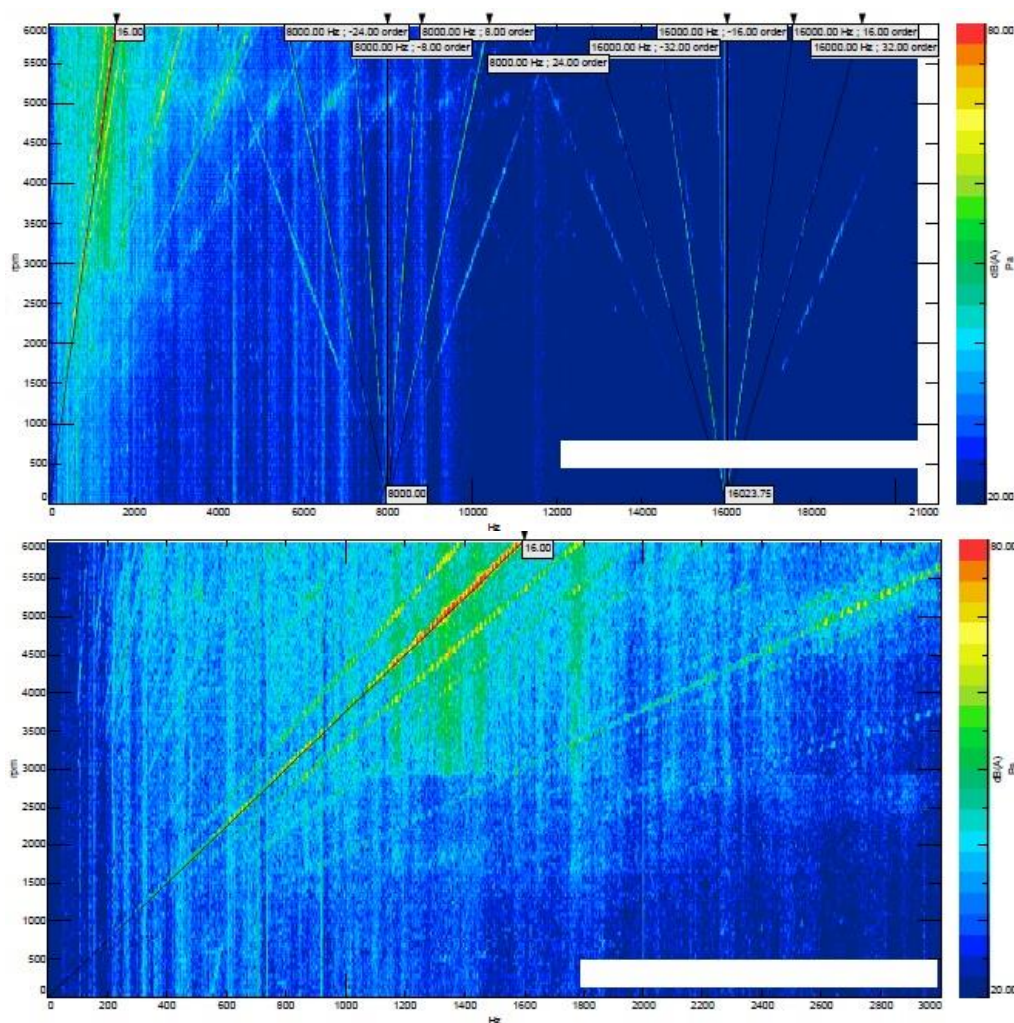


Figure 4.24 Waterfall diagrams of sound pressure

As can be seen in Figure 4.23, the sound pressure and acceleration amplitude increase rapidly for motor speed above approximately 4000rpm. The sound above 5000Hz mainly comes from the electric swishing frequency of 8000Hz with related orders. Listening only to the sound above 5000Hz may not be so strong but very unpleasant sound. The highest sound in the test is about 103dB. And in different position, the

vibration amplitude seems to be different. Compare with the simulation results, SPL is approximately 120dB in the position with radius of 0.5m under 4800rpm. Whereas, 80Hz of rotor is also the disturbance frequency as compared with the simulated results. Consider the distance attenuation, sound pressure shares the same tendency with experiment.

The waterfall diagram shows that vibration and noise generates most within low frequency range. And for the 16 poles electrical machine, 1600Hz is the frequency with highest SPL of 80dB. In ANSYS results, 1205.5 is the frequency with highest vibration response for pure stator model.

## 5 Sensitivity Analysis

Sensitivity analysis is used in optimizing design to qualitatively or quantitatively evaluate the influence of parameters variation on the output variables. (XU Chonggang, HU Yuanman,2004) It is classified into two groups: local sensitivity analysis which examines the impact of one parameter at a time; global sensitivity analysis who checks the response on the output results over the variations of all parameters. Main influence factor can be achieved by comparing the results of local sensitivity analysis and the interaction of different parameters can be got from global analysis. The main methods for global sensitivity analysis include Morris' method, Fourier Amplitude Sensitivity Evaluation, multivariate regression and so on. While the method for local sensitivity analysis is easier and is already used worldwide in optimal designing. But the disadvantage is time-consuming since only one parameter can be changed at one time and simulations should be done one by one. Here, local sensitivity analysis is used to compare the proportion of structure parameters' influence on stator vibration.

### 5.1 Local sensitivity analysis method

The mathematical equation of local sensitivity analysis is basically the derivative of the output variables with respect to the input parameters:

$$s = (F)_i = \frac{\partial F(x)}{\partial x_i} \text{ or } s = \frac{\Delta F(x)}{\Delta x_i} \quad (5.1)$$

where  $s$  represents sensitivity of one parameter;  $F(x)$  is the output parameters which is a differentiable function to the input parameter  $x$ . Here,  $x$  is consisted of stator back thickness which is simulated by changing the outer diameter of the stator, shell thickness, air gap, stator teeth thickness and stator tip width. For air gap length variation, the stator part keeps constant while the radius of rotor is changed in order to keep other stator geometry unvarying. In addition, changing stator tip width and length of teeth tip gap is the same. These parameters definition in the model is shown in Figure 5.1.

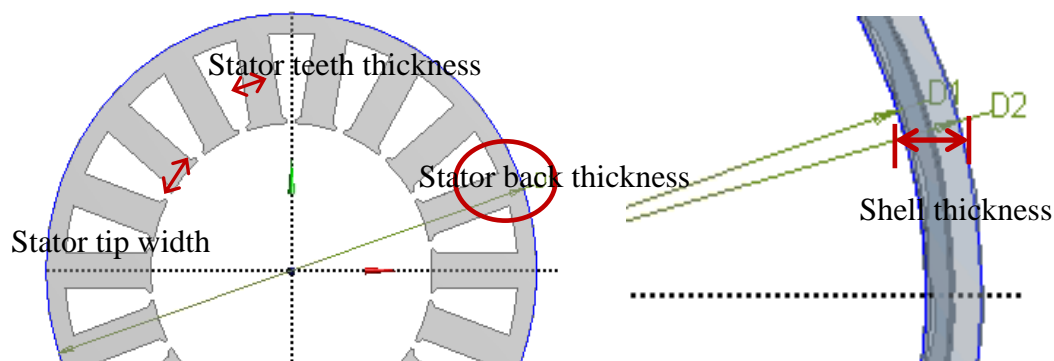


Figure 5.1 Input parameters of local sensitivity analysis

Sensitivity analysis for structure parameter includes two aspects, static and dynamic. Among them, dynamic one studies the eigenvalues, eigenvectors and dynamic response of one model while static one analyzes the displacement, stress and so on. In this project, it is sorted into dynamic sensitivity analysis, since the analyzed parameter is the resonance frequency which is a dynamic response of the pressure. Therefore, a new vibration response is generated when changing structure parameters every time. Then sensitivity value can be got from equation (5.1).

Reason why chooses these parameters is that amplitude or phase of electromagnetic force excitation depends on the geometry of slots, length of air gap, winding arrangements, etc. Like the impact of air gap on magnetic flux density is significant which is mentioned in chapter 2. Especially the tooth tips are the interface for forces to deliver energy into the structure, so those parameters connected to geometry of tooth tips are considered and calculated.

## 5.2 ANSYS Sensitivity analyse method

Parameters Correlation in ANSYS Workbench can be used to do a general sensitivity analysis of the geometry influence. Parameterize the input structure parameters and the concerned output variables. In this section, model of parameterize geometry need to be simulated separately to save time and improve the accuracy. In addition, the interaction between different geometry size, like the outer diameter of stator and the inner shell diameter leads to error of simulation.

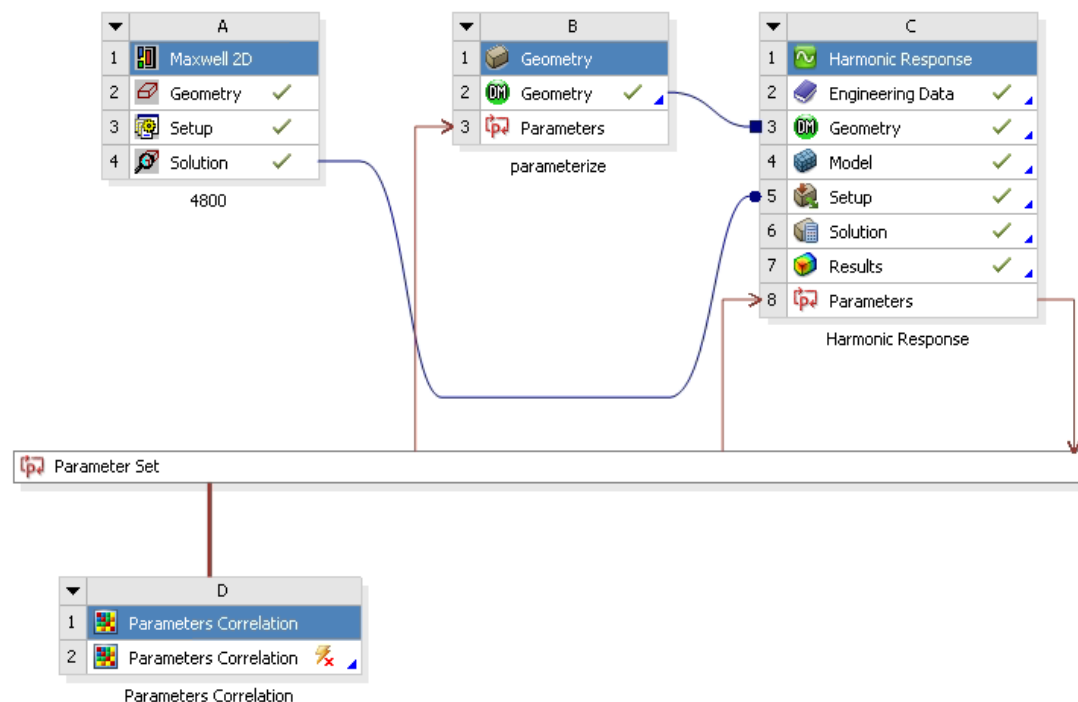


Figure 5.2 ANSYS Sensitivity analyse method

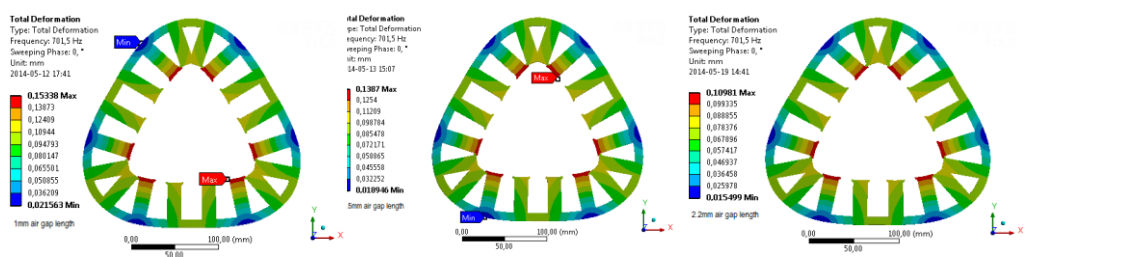
The parameterized input parameters include stator diameter, extrude length, teeth thickness and stator tip radius while resonance frequency is set as an output data for dynamic sensitivity evaluation. Analyze frequency range is set separately for resonance frequency range correspondence to each mode shape that means simulation for every scale is isolated. Lower and upper bound of the inputs is set in Parameters Correlation module and choose 'sensitivity' to do the calculation. However, this method is not very efficient and accurate, since the 2D structure parameters in Maxwell cannot change related to the bound settings. But the force amplitude will change in a small scale when structure is changing. Moreover, computer needs a huge memory to store this simulation results because one single parameter's calculation needs about 10G space or even more.

## 5.3 Local sensitivity analyse results

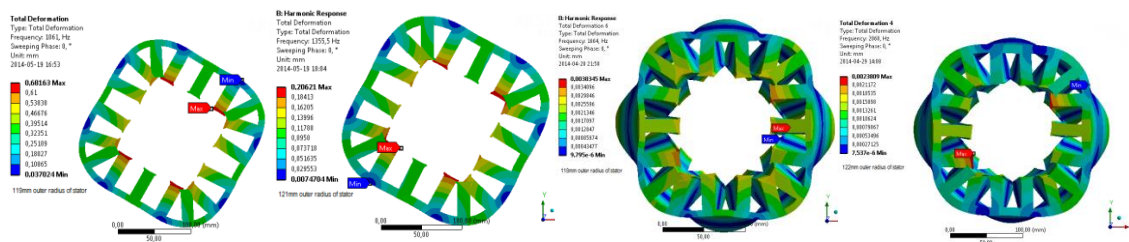
Table 5.1 Sensitivity of different structure parameter

Mode shape	Stator back thickness(Hz /mm)	Air gap (Hz /mm)	Stator teeth thickness(Hz /mm)	Stator tip width(Hz /mm)	Shell thickness (Hz /mm)
1st	33.89	0.401786	-2	0.5	18.625
2nd	85.25	-0.1875	-5.25	1.75	39.75
3rd	146.5	0.1875	-8.875	2.5	32.625
4th	203.5	0.375	-10.375	5.25	81.25
5th	243.25	-0.83	-7.75	7.25	-81.25
6th	288.8	0.021	-2.5	12.25	-25
7th	270.8	-1.083	3.625	44.25	22.5
8th	128.35	-0.3125	-65.125	5.5	12.5

As shown in table 5.1, stator back thickness is the most sensitivity value within the stator core geometry. The frequency influence on 4th,5th,6th and 7th plane mode already achieves more than 200Hz per millimeter. Even the relatively weak impact on the first three mode shape is much greater than the other three variables. Compare the sensitivity of the last three parameters; stator tip width has great impact on correspondence frequency of the 6th and 7th mode, while stator teeth thickness affects more on high frequency like the 8th vibration response. However, air gap length seems having no influence on the frequency response for every deformation mode shape. But as mentioned in Chapter 2, air gap decreasing leads to significantly growing of the electromagnetic force excitation because of the dramatically increased flux density inside the air gap. As a result, deformation of every shape enhances a lot with the reduction of air gap length shown in Figure 5.3(a).



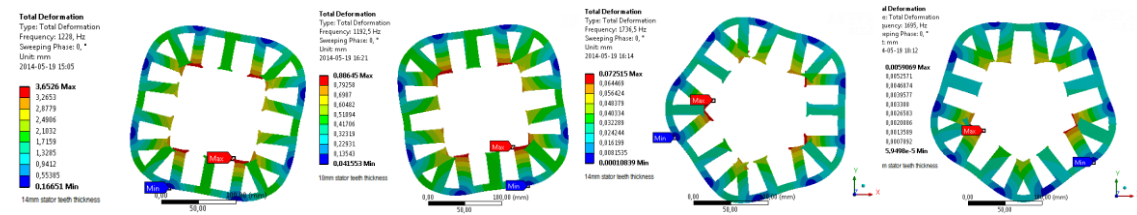
(a) Deformation for air gap difference



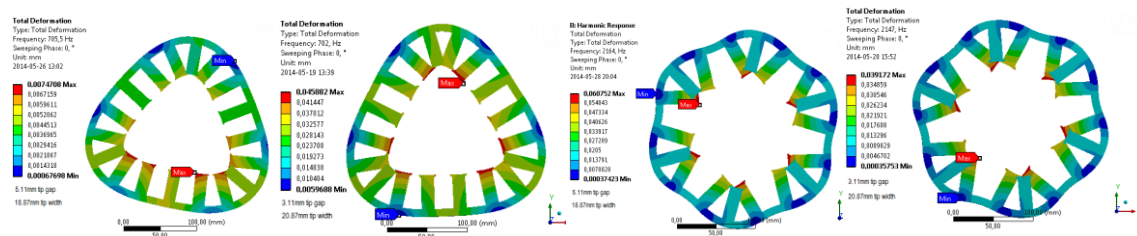
(b) Deformation for stator back difference

Figure 5.3 Impacts on deformation for different parameters

Besides, other parameters also affect the deformation response, like increasing the stator back, deformation can be reduced including the asymmetric shape in Figure 5.3(b). With the increase of stator teeth thickness and tip gap, amplitude of deformation for every mode shape reduces which is shown in Figure 5.4. Here, when stator tip gap grows, the stator tip width decreases. Therefore, the surface area reduces as well as the pressure excitation acted on the stator tip surface. The shell thickness is also an important influence factor for the resonance frequency like showing in the fifth column of table 5.1. Sensitivity value is great especially for the 4<sup>th</sup> and 5<sup>th</sup> radial vibration mode shape.



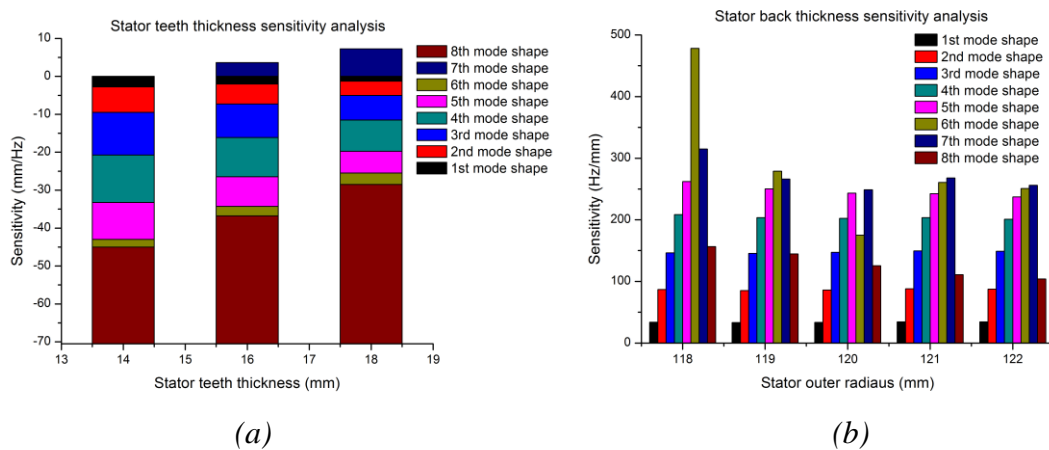
a) Deformation for stator teeth difference



b) Deformation for difference of stator tip width

Figure 5.4 Impacts on deformation for different parameters

It is worth mentioning that the sensitivity value in Table 5.1 is an average number of the derivate in every interval. And the exact frequency value is shown in Appendix 4, whereas, the relationship between inputs and outputs is not at all linear. So these values can only be used to compare the extent of importance of the structure parameters, but cannot be used to estimate the variation tendency. In Figure 5.5 gives the variation relation between inputs and outputs. Here, stator teeth increases from 14mm till 18mm; stator exterior diameter is changed from 236mm to 244mm. While air gap length enlarges 1mm every step and tooth tip gap is adjusted from 3.11 till 5.11mm. At last, shell thickness is altered as 262mm,264mm and 266mm to analyze the sensitivity.



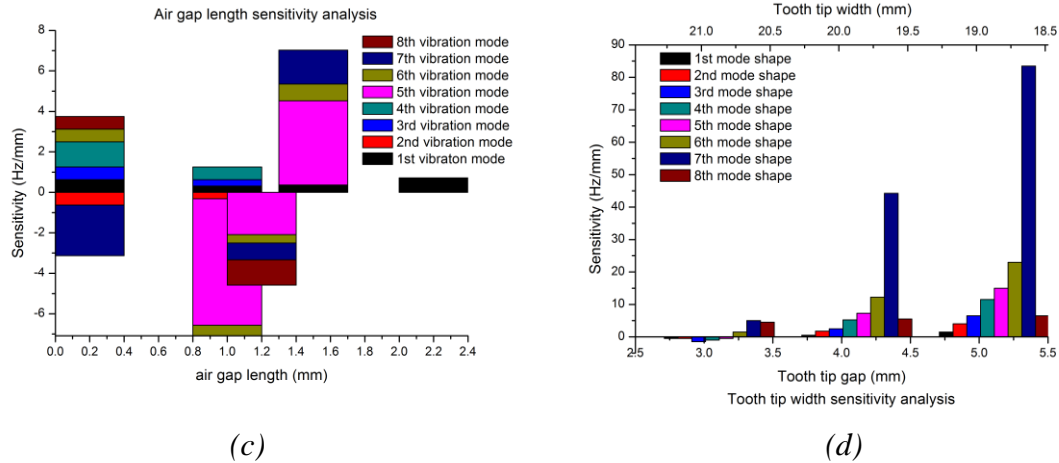


Figure 5.5 Sensitivity trends for stator back, air gap, teeth and tips

(a) Stator teeth thickness sensitivity; (b) Stator outer diameter (stator back thickness) sensitivity; (c) Air gap length sensitivity; (d) Tooth tip width sensitivity

As shown in the stack column chart of stator teeth thickness sensitivity, all frequency except the resonance for the 7th plane mode changes into the negative direction, which means frequency trends to decrease when enlarging teeth thickness value. For the bar chart of stator back sensitivity, the growth rate for every 1mm increasing is different, but frequency will enhance at a steady state with the increasing of the exterior diameter of stator core. Also the growth rate for the corresponding frequency of first five mode shapes is an average value, but for high frequencies, the growth rate curve becomes nonlinear. In addition, air gap length adjustment seems having irregular trends. Yet it is because all the frequency changes little and even stays constant or the deviation of computation. In Figure 5.4(d), with the risen of tooth tip width, the drop rate becomes less and less and even turns adverse at 21mm.

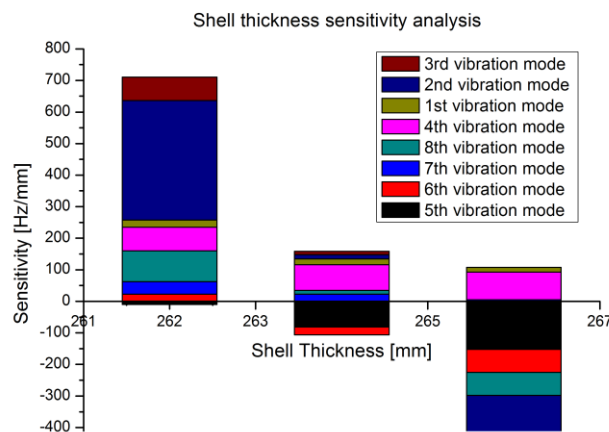


Figure 5.5 Shell thickness sensitivity analysis

As shown in Figure 5.5, 262mm and 266mm have a great influence on the 2<sup>nd</sup> frequency and the changing rate is nonlinear and has both positive and negative sensitivity value. Local sensitivity analysis is used to compare the static sensitivity of every structure parameters, but the interaction between geometry is ignored. For further study, global sensitivity analyze method can be introduced.

## 6 Conclusion

Electromagnetic force is the most important vibration source of an electrical machine in this project. It is generated by the magnetic flux within the air gap. These forces mainly act on the surface of stator tip and will cause the radial vibration of stator.

By using Finite Element Methods, the electromagnetic effect and vibration response of an electrical machine is solved in some extent. Also local sensitivity analysis of stator and cylinder geometry is finished to compare the influence extent of each structure parameter. Here are the main results coming from this project.

- I. Vibration within 0-5000Hz is the most concentrated frequency range of this EM prototype, since in low frequency range, radial electromagnetic force causes serious radial vibration who is the most importance vibration mode shape of stator core.
- II. For the rotation speed of 4800rpm, the electric frequency 640Hz is a disturbance frequency for this motor structure which will increase the vibration response of the simulated model.
- III. Fixed support of the outer cylinder enhances the stiffness of the system. Therefore, resonance frequency for each mode shape will be improved. As well as increasing the contact area with cooling system shell, the stiffness will increase, either.
- IV. Air gap length influences force excitation and vibration amplitude seriously, but not affects system characteristics, that means frequency is not influenced. At the same time, other structure parameters have no great impact on the changing of electromagnetic force excitation.
- V. For sensitivity analysis, stator back thickness and shell thickness influences resonance frequency seriously, while other geometry only has small impact.

### 6.1 Discussion

The vibration and acoustic performance for the part of electrical machine has already been finished in this project. However, there are still problems leaving behind and more future work to do.

The first thing is that there is some inaccuracy caused by the assumption and the simplified model in the winding model. The assumption that slots are solid entities filling with copper is wrong. This simplified model is inappropriate since the stiffness of wrapped copper line is totally different as an entity. This causes the mistake of resonance frequency. To solve this problem, an equivalent material method or dynamic elastic modulus can be applied.

Second, the experimental data is not directly comparable with the simulation results, because the test speed of the electrical machine is a transient process from 0rpm to 6000rpm and the torque cannot be confirmed at that time. However, the simulation from ANSYS Maxwell is at one steady speed with a responding torque and power. Hence, the results can only be used to estimate the roughly accuracy of this simulation.

Last but not least, structure and geometry difference lead to the changing of resonance frequency and vibration response. In this project, only two shell model, one winding model and local sensitivity is calculated. The chassis and other part of this prototype has not been simulated, as well as other force excitation. Furthermore, local sensitivity analysis does not involve the interaction between geometry parameters when changing only one parameter at one time.

## 6.2 Future scope

From the several problems in discussion part, the future work includes:

- a) Simulation of a new winding model using equivalent material method or dynamic elastic modulus. Here, dynamic elastic modulus is achieved from the test of a wrapped copper line.
- b) Global sensitivity analysis can be introduced to estimate the whole influence of geometry.
- c) Function extension such as connecting with GT-SUITE to calculate the force excitation within 0rpm to 6000rpm and simulate the vibration response under a transient process. Otherwise, a new test under steady working speed can be done to compare with the simulation results. In addition, another function extension such as a thermal model can be built to estimate the vibration under high temperature, since material will be expanding in a high temperature under high rotating speed.
- d) Optimization design of electrical machine can be done in the future work after the global sensitivity analysis.
- e) Rotor vibration is mainly caused by the inertia of rotor mass and the support position. Hence, the simulation process is totally different from stator vibration. In reality, this rotor is connected with a gear box to provide torque to the shaft of gear box. Therefore, the mechanical force excitation from the gear needs to be considered in the future simulation of rotor dynamic.

## 7 Reference

- [http://en.wikipedia.org/wiki/Resonance\\_frequency#Mechanical\\_and\\_acoustic\\_resonance,20140516](http://en.wikipedia.org/wiki/Resonance_frequency#Mechanical_and_acoustic_resonance,20140516)
- [http://en.wikipedia.org/wiki/Sound\\_pressure\\_level#Sound\\_pr](http://en.wikipedia.org/wiki/Sound_pressure_level#Sound_pr)
- <http://www.infomine.com/investment/metal-prices/crude-oil/all/,2014-04-15>
- Svenska Petroleum Institute, <http://www.spi.se>
- A.J.Ellison, B.Sc.(Eng.). (1968): Acoustic Noise and Vibration of Rotating Electric Machines. *PROC.IEE*, Vol.115, No.11, November 1968.
- A.J.Ellison, D.Sc.(Eng.). (1971): Natural Frequencies of Stators of Small Electric Machines. *PROC. IEE*, Vol. 118, No. 1, JANUARY 1971
- Anwar, M.N. and Husain, I. (2000): Radial Force Calculation and Acoustic Noise Prediction in Switched Reluctance Machines. *Industry Applications, IEEE Transactions*, Vol. 36, Issue: 6: 2000. pp. 1589-1597.
- Banharn Sutthiphornsombat. : *Prediction of Torque and Radial Forces in Permanent Magnet Synchronous machines using Field Reconstruction Method*. Master Thesis. Department of Electrical Engineering, University of Texas.
- Bashir Mahdi Ebrahimi, Mohammad Etemadrezaei. (2011): Dynamic eccentricity fault diagnosis in round rotor synchronous motors. *Energy Conversion and Management*, Vol. 52, No. 5, May 2011, pp. 2092-2097.
- Dimitri Torregrossa, François Peyraut. (2010): A New Passive Methodology for Reducing the Noise in Electrical Machines: Impact of Some Parameters on the Modal Analysis. *IEEE Transactions on Industry Applications*, Vol. 46, No. 5, September/October 2010
- Fanhui Zhang, Shuguang Zuo.(2012): Analysis of Influencing Factors on Stator's Vibration Characteristics And Optimization Design of Drive Motor[J]. *China Academic Journal Electronic Publishing House*, Vol. 40, No. 9, 2012. (in Chinese).
- Hong-Seok Ko, Kwang-Joon Kim. (2004): Characterization of Noise and Vibration Sources in Interior Permanent-Magnet Brushless DC Motors. *IEEE Transactions on Magnetics*, Vol. 40, No. 6, November 2004. Pp. 3482-3489.
- Hyeon-Jae Shin, Jang-Young Choil.(2012).: Analysis on Electromagnetic Vibration Source Permanent Magnet Synchronous Motor for Compressor of Electric Vehicles. Department. of Electrical Engineering, Chungnam National University, *IEEE Vehicle Power and Propulsion Conference*. October 2012.
- Janne Roivainen. (2009): *Unit-wave Response-based Modelling of Electromechanical Noise and Vibration of Electrical Machines*. Doctoral Dissertation Department of Electrical Engineering, Helsinki University of Technology, June 2009.
- João Pedro A. Bastos Nelson Sadowski. (2003): *Electromagnetic Modelling by Finite Element Methods*. Marcel Dekker, Inc, 2003, pp. 35-285.
- John F. Cochran, Bretislav Heinrich. (2004): *Applications of Maxwell's Equations*. Simon Fraser University, Burnaby, B.C., Canada. December 2004.
- Jordan H, Muller-Tomfelde H. (1961): Akustische Wirkung der Schragung bei Drehstrom-Asynchronmaschinen mit Kafiglaufnern. *Elektrotecli Z.*, 1961, pp. 788-792.

- Koen Delaere, Ronnie Belmans. (2003): Influence of Rotor Slot Wedges on Stator Currents and Stator Vibration Spectrum of Induction Machines: A Transient Finite-Element Analysis. *IEEE Transactions on Magnetics*, Vol. 39, No. 3, May 2003, pp. 1492-1498.
- Lakshmikanth. S\*, Natraj. K.R. (2012): Noise and Vibration Reduction in Permanent Magnet Synchronous Motors –A Review. *International Journal of Electrical and Computer Engineering*, Vol.2, No.3, June 2012, pp. 405-416
- Liyan Wang, Lixiu Zhang. (2011): Simulation Analysis on the Influence of Magnetic Field Distribution Caused by Motor Spindle Air-gap. *International Conference on Electronic & Mechanical Engineering and Information Technology*. August 2011. pp. 215-218
- M.E.H. Benbouzid, G. Reyne. (1993): Finite Element Modeling of a Synchronous Machine :Electromagnetic Forces and Mode Shapes. *IEEE Transactions on Magnetics*, Vol. 29, No. 2, March 1993, pp. 2014-2019.
- Pavel Kukula, Cestmír Ondrušek. (2007): Electric Machine Vibration Analysis. *Konference diplomových prac í 2007*.
- Ping Liu, Zeqing Wan. (2007): Improvement of Equivalent elastic modulus of Composite materials. *Journal of Yangzhou University (natural science edition)*, Vol. 10, No. 1, February 2007.
- Rakib Islam, Iqbal Husain. (2010): Analytical Model for Predicting Noise and Vibration in Permanent-Magnet Synchronous Motors. *IEEE Transactions on Industry Applications*, Vol. 46, No. 6, November/December 2010, pp. 2346-2352.
- Robert D.Cook, David S. Malkus. (1989): *Concepts and Applications of Finite Element Analysis*. University of Wisconsin, 3<sup>rd</sup> edition, 1989.
- Rothert H. (1957): Magnetisch erregte Schwingungen an Gleichstrommaschinen, *VDI Ber.*, 1957, pp. 39-44
- Sanda Victorinne Paturca, Mircea Covrig. (2006): Direct Torque Control of Permanent Magnet Synchronous Motor (PMSM) – an approach by using Space Vector Modulation (SVM). Department of Materials, University Politehnica of Bucharest, *Proceedings of the 6th WSEAS/IASME Int. Conf. on Electric Power Systems, High Voltages, Electric Machines*, Tenerife, Spain, December 16-18, 2006.
- Senlin Huang, Hengfeng Chen.: *Rotor Dynamics Analysis of An Electric Machine*. TECO FA Global Wuxi R&D Center.
- Steffen Peters. (2011): Airborne Sound of Electrical Machines using Symmetric Matrices in ANSYS 14. *ANSYS Conference & 29. CADFEM Users' Meeting, October 2011*.
- Tianyu Wang, Fengxiang Wang. (2007): Vibration and Modal Analysis of Stator of Large Induction Motors [J]. *Proceedings of the CSEE*, Vol. 27, No. 12, April 2007 (in Chinese).
- Wang X H, Li Q F. (2003): Analytical calculation of air-gap magnetic field distribution and instantaneous characteristics of brushless DC motors [J]. *IEEE Transactions On Energy Conversion*, Vol. 18, No. 3. 2003. pp. 424-432.
- William Cai, P Pillay. (2001): Resonance Frequencies and Mode Shapes of Switched Reluctance Motors [J]. *IEEE Transactions on Energy Conversion*. 2001. pp. 44-47.

- William Cai, P Pillay. (2001): Low Vibration Design of SRMs for Automotive Applications Using Modal Analysis [C]. *Electric Machines and Drives Conference*. 2001.
- William Cai, P Pillay. (2002): Impact of Stator Windings and End-bells on Resonant Frequencies and Mode Shapes of Switched Reluctance Motors [J]. *IEEE Transactions on Industry Applications*. Vol. 38, No. 4, 2002, pp.1027-1036.
- XU Chonggang, HU Yuanman. (2004): Sensitivity analysis in ecological modeling. *Chinese Journal of Applied Ecology*. Vol. 15, No. 6. June 2004, pp. 1056-1062.
- Yan Li, Shuangpeng Li. (2013): Noise and Vibration Characteristics Analysis on Different Structure Parameters of Permanent Magnet Synchronous Motor. *International Conference on Electrical Machines and Systems*, Busan, Korea. October.26-29, 2013. pp. 46-49.
- Yie Zhong, Zheng Wang. (1987): *Rotor Dynamics*. Tsinghua University Press: Beijing (in Chinese).
- Z Q Zhu, D Howe. (1989): Effects of End Shields and Rotor on Natural Frequencies and Modes of Stator of Small Electrical Machines [C]. *Fourth International Conference on Electrical Machines and Drives*. London,1989.pp 232-236.

## 8 Appendix 1

```
'-----  
' Script Recorded by Ansoft Maxwell Version 2014.0.0  
' 12:38:31 apr 01, 2014  
'-----  
  
Dim oAnsoftApp  
Dim oDesktop  
Dim oProject  
Dim oDesign  
Dim oEditor  
Dim oModule  
Set oAnsoftApp = CreateObject("AnsoftMaxwell.MaxwellScriptInterface")  
Set oDesktop = oAnsoftApp.GetAppDesktop()  
oDesktop.RestoreWindow  
  
projName = "MC2"  
designName = "Orig"  
  
' For parameter 1  
name1 = "NAME:Is"  
unit1 = "A"  
start1 = 50  
stop1 = 100  
step1 = 50  
  
' For parameter 2  
name2 = "NAME:thetaA"  
unit2 = "deg"  
start2 = 90  
stop2 = 180  
step2 = 10  
  
Set oProject = oDesktop.SetActiveProject("split_statortip_cal")  
Set oDesign = oProject.SetActiveDesign("Orig")  
  
'For param2 = start2 To stop2 Step step2  
For param2 = start2 To stop2 Step step2 'Each param2 As Integer In values2
```

```

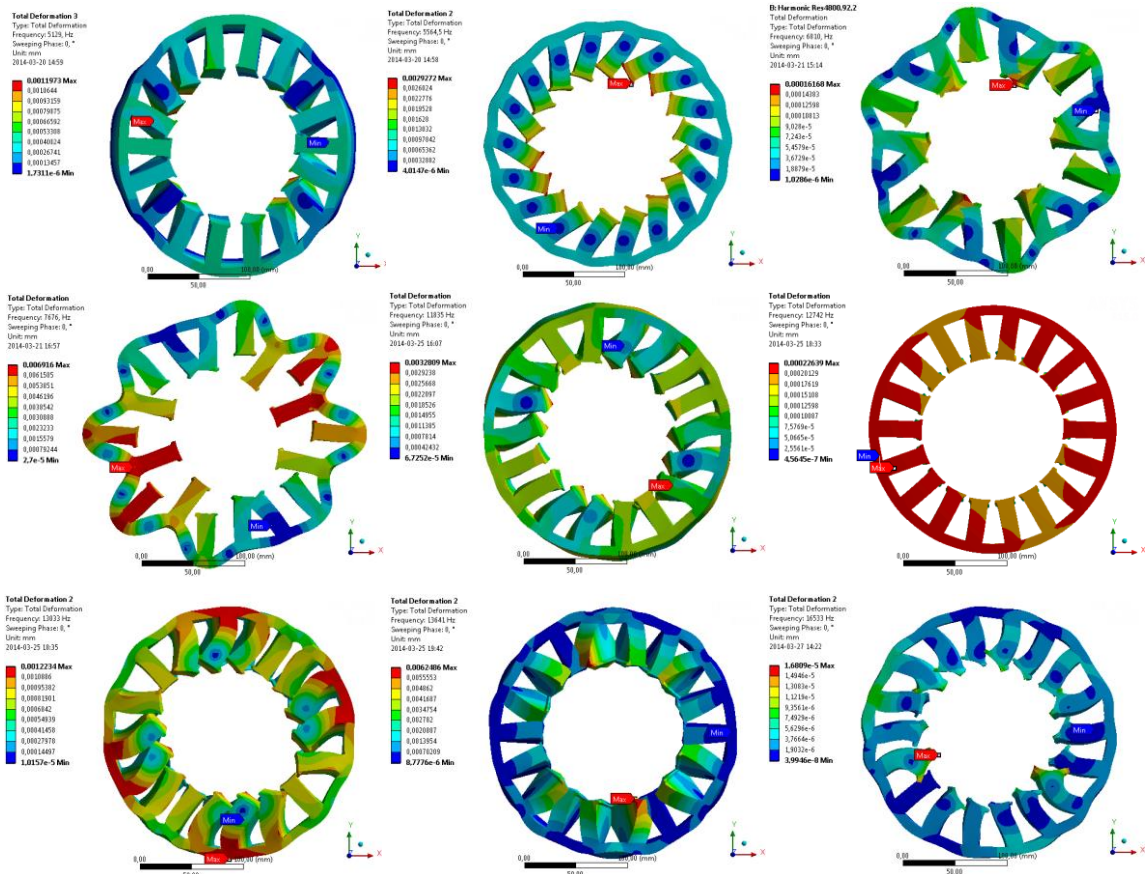
msg2 = param2 & unit2
oDesign.ChangeProperty Array("NAME:AllTabs", Array("NAME:LocalVariableTab",
Array("NAME:PropServers", _
"LocalVariables"), Array("NAME:ChangedProps", Array(name2, "Value:=", msg2))))
For param1 = start1 To stop1 Step step1
msg1 = param1 & unit1
oDesign.ChangeProperty Array("NAME:AllTabs", Array("NAME:LocalVariableTab",
Array("NAME:PropServers", _
"LocalVariables"), Array("NAME:ChangedProps", Array(name1, "Value:=", msg1))))
oDesign.Analyze "Setup1"
oProject.Save
Next
Next

```

# Appendix 2

Table 8.1 Resonance frequency for pure stator vibration in high frequency range

Mode shape	Resonance frequency(Hz)
9th	4166
10th	5129
11th	5564.5
12th	6810
13th	7676
14th	11835
15th	12742
16th	13033
17th	13641
18th	16533



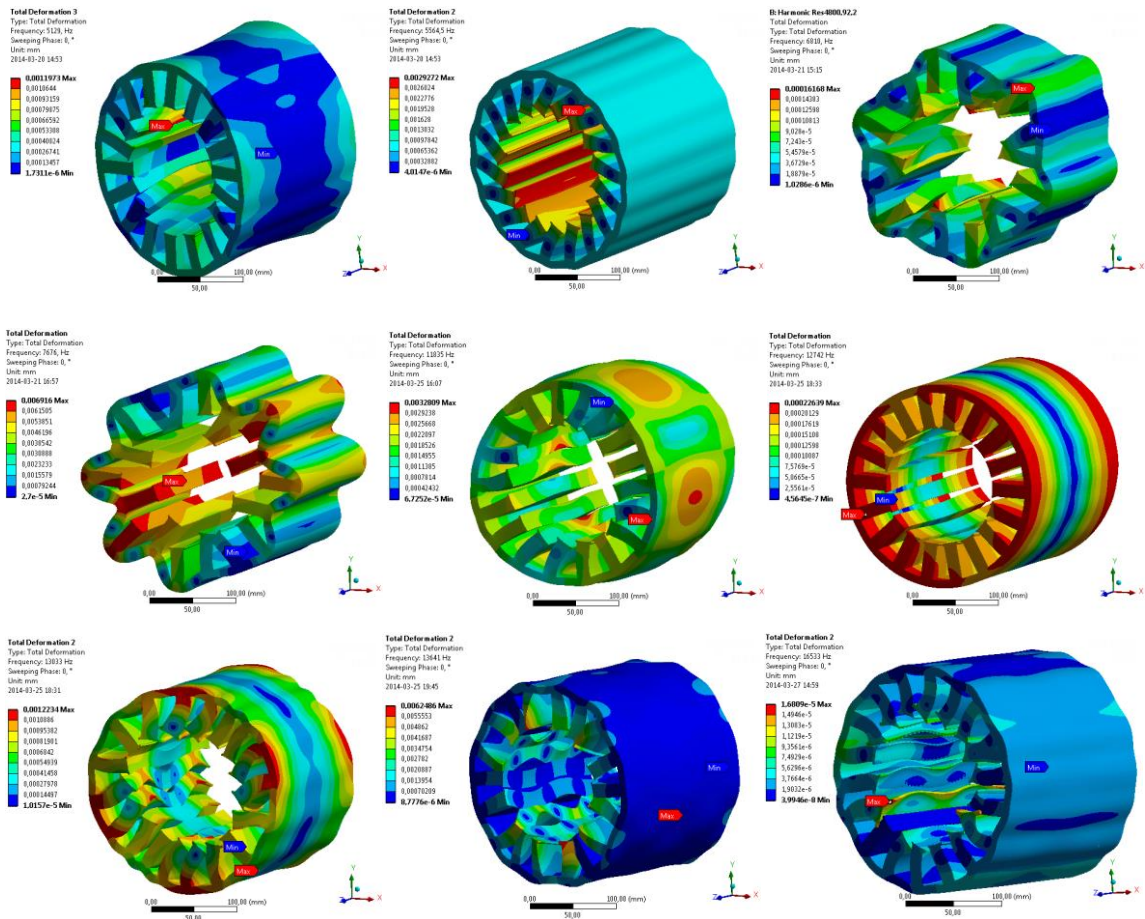


Figure 8.1 Radial and shear vibration mode shape

# 10 Appendix 3

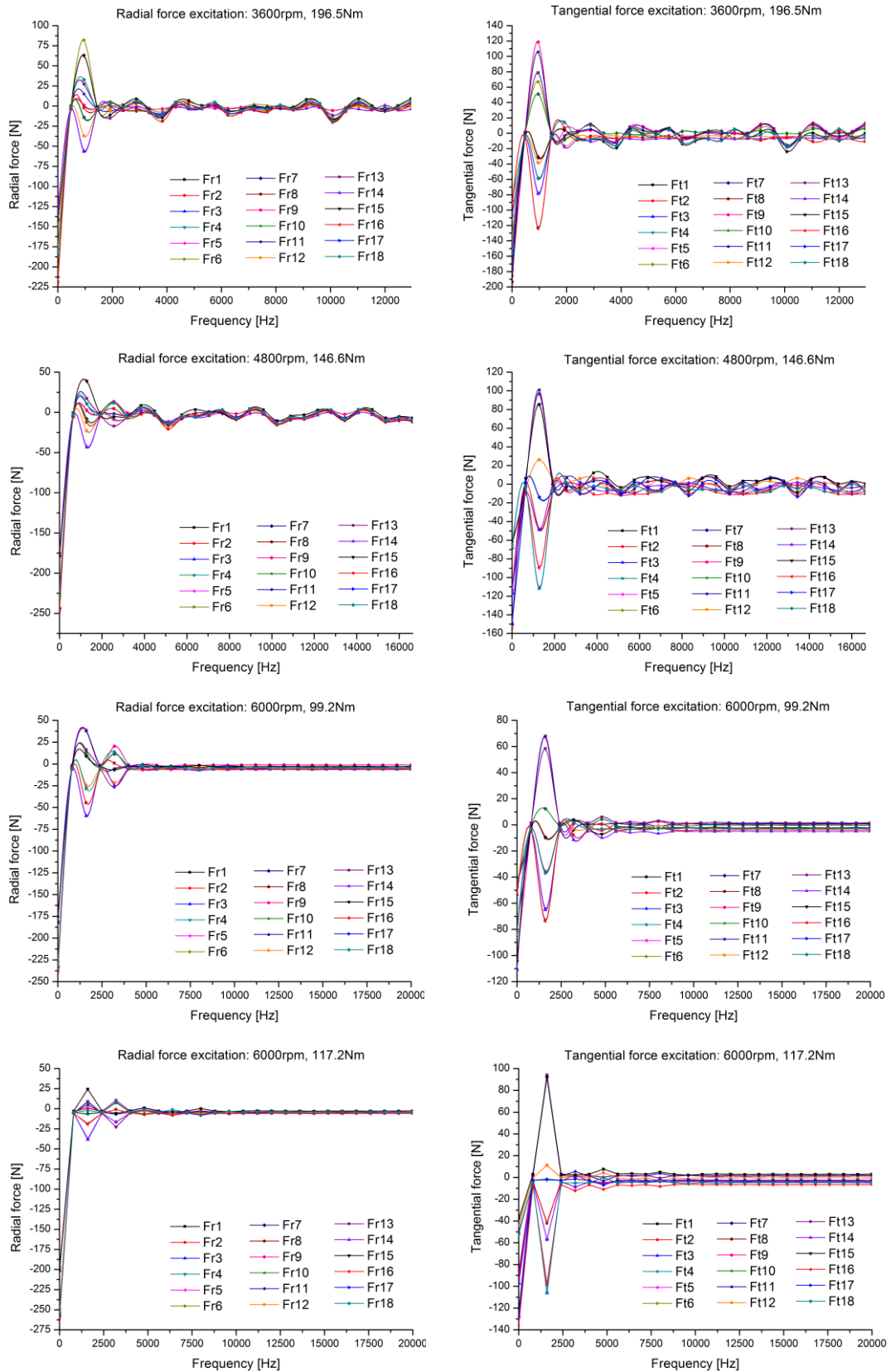


Figure 8.2 Force excitations under different operating points

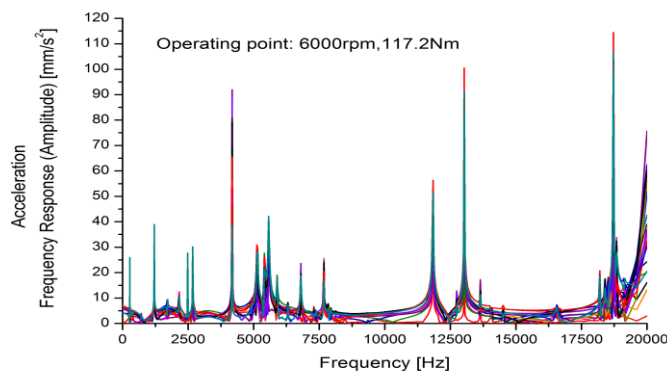
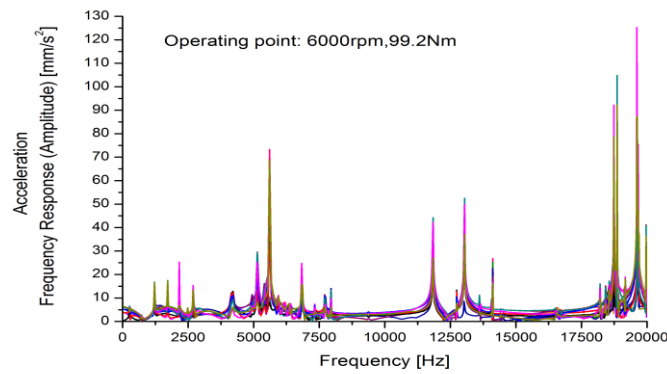
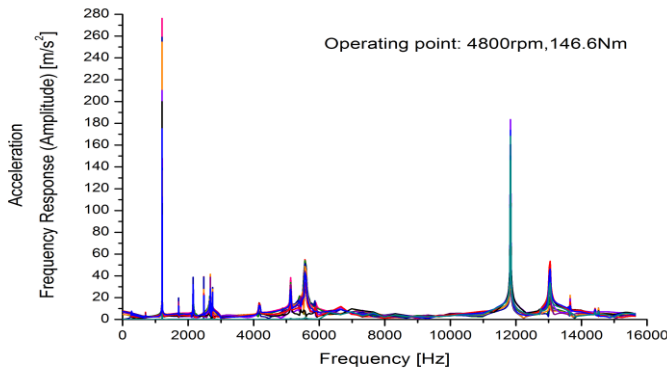
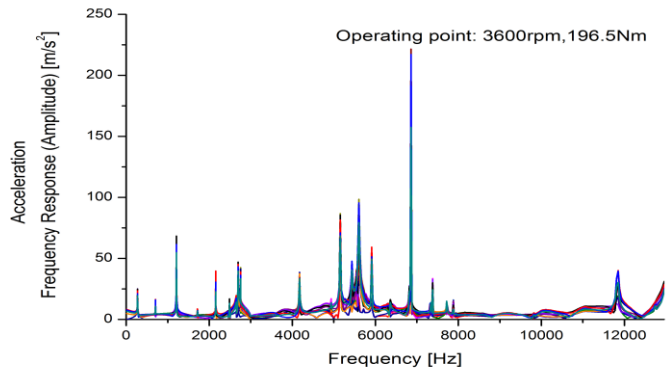


Figure 8.3 Frequency response of acceleration amplitude

## Appendix 4

Stator back thickness						Air gap length				
Mode shape	118mm	119mm	120mm	121mm	122mm	1mm	1,2mm	2,2mm	1,5mm	0,2mm
1st	206.2	240	272.5	307	341.5	272.5	272.5	272.5	272.5	272.5
2nd	531	618	701.5	790	877.5	701.5	701.5	701.5	701.5	701.5
3rd	914.5	1061	1205.5	1355.5	1504.5	1205.5	1205.5	1205.5	1205.5	1205.5
4th	1304.5	1513	1711.5	1917.5	2118.5	1711.5	1711.5	1711.5	1711.5	1711.5
5th	1648.5	1910.5	2149	2397	2634	2151.5	2149	2151.5	2151.5	2151.5
6th	1920.5	2398.5	2478.5	2749	3000	2479	2478.5	2479	2479	2479
7th	2144.5	2459.5	2677	2957	3213	2678	2677	2678	2678	2678
8th	3886	4042.5	4175.5	4293.5	4397.5	4175.5	4175.5	4175.5	4175.5	4175.5

shell thickness				stator teeth thickness			stator tip thickness		
Mode shape	262mm	264mm	266mm	14mm	16mm	18mm	(3.11)20,87mm	(4.11)19.87mm	(5.11)18.87mm
1st	800.5	845	875	278	272.5	270	273	272.5	274
2nd	1047	1805	1100	715	701.5	694	702	701.5	705.5
3rd	2631.5	2780	2675	1228	1205.5	1192.5	1207	1205.5	1212
4th	2900	3050	3225	1736.5	1711.5	1695	1712.5	1711.5	1723
5th	3850	3830	3525	2168.5	2149	2137.5	2149.5	2149	2164
6th	3950	3995	3850	2482.5	2478.5	2472.5	2477	2478.5	2501.5
7th	4035	4115	4125	2667	2677	2681.5	2672	2677	2760.5
8th	4775	4970	4825	4315	4175.5	4054.5	4171	4175.5	4182